RESEARCH ARTICLE

Figures and figure supplements

Lipid transfer from plants to arbuscular mycorrhiza fungi

Andreas Keymer *et al*

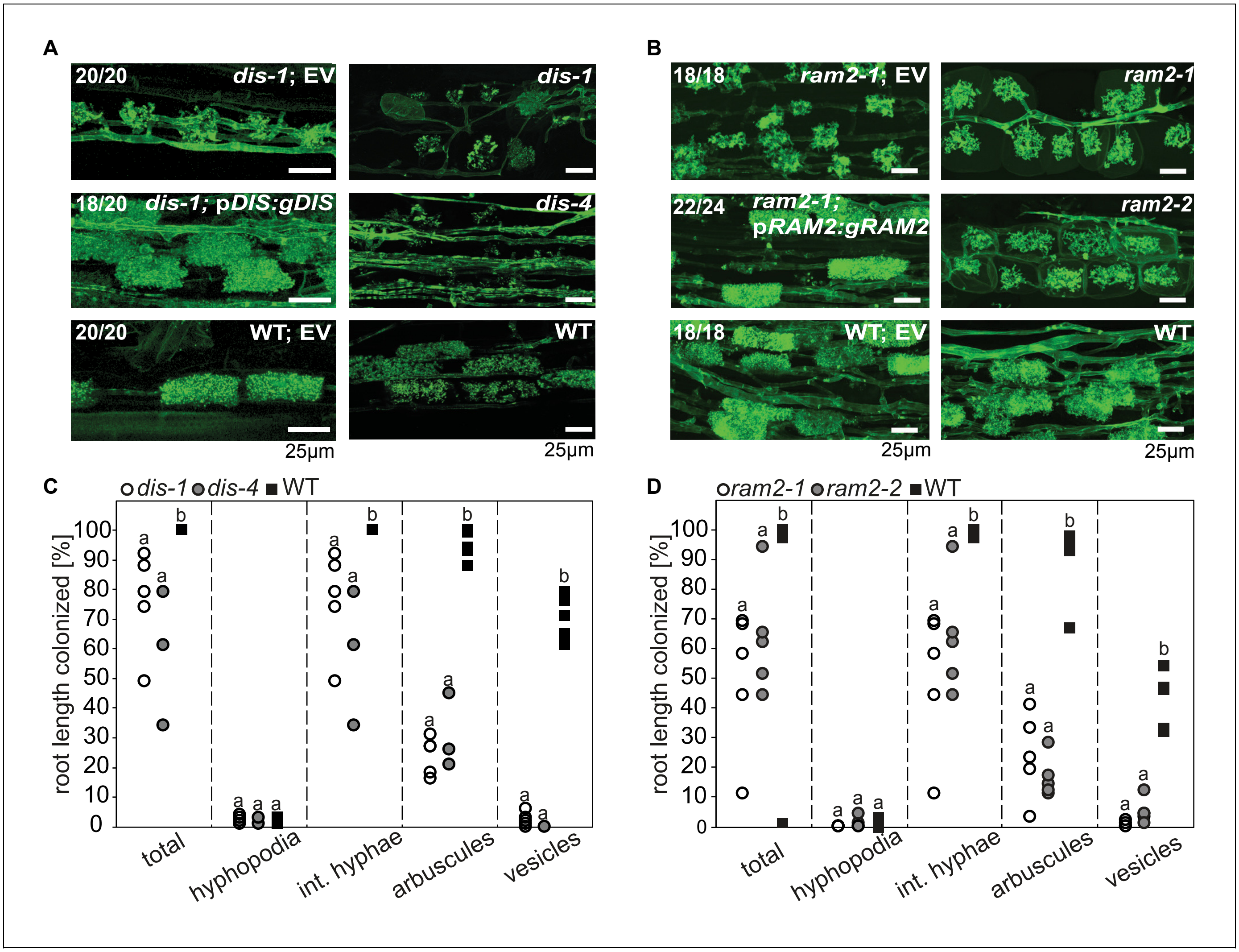

Figure 1. *DIS* and *RAM2* are required for arbuscule branching and vesicle formation. Arbuscule phenotype and complementation of *dis* (**A**) and *ram2* (**B**) mutants. The fungus was stained with wheat-germ agglutinin (WGA)-AlexaFluor488. (**C-D**) Percent root length colonization of *dis* (**C**) and *ram2* (**D**) mutants as compared to wild-type. Different letters indicate significant differences among treatments (ANOVA; posthoc Tukey). (**C**): n = 13; $p \leq 0.1$, $F_{2,10} = 8.068$ (total & int. hyphae); $p \leq 0.001$ $F_{2,10} = 124.5$ (arbuscules); $p \leq 0.001$, $F_{2,10} = 299.1$ (vesicles) (**D**): n = 15; $p \leq 0.1$, $F_{2,12} = 10.18$ (total & int. hyphae); $p \leq 0.001$ $F_{2,12} = 57.86$ (arbuscules); $p \leq 0.001$, $F_{2,12} = 72.37$ (vesicles). (**A-D**) Plants were inoculated with *R. irregularis* and harvested at 5 weeks post inoculation (wpi).

DOI: 10.7554/eLife.29107.003

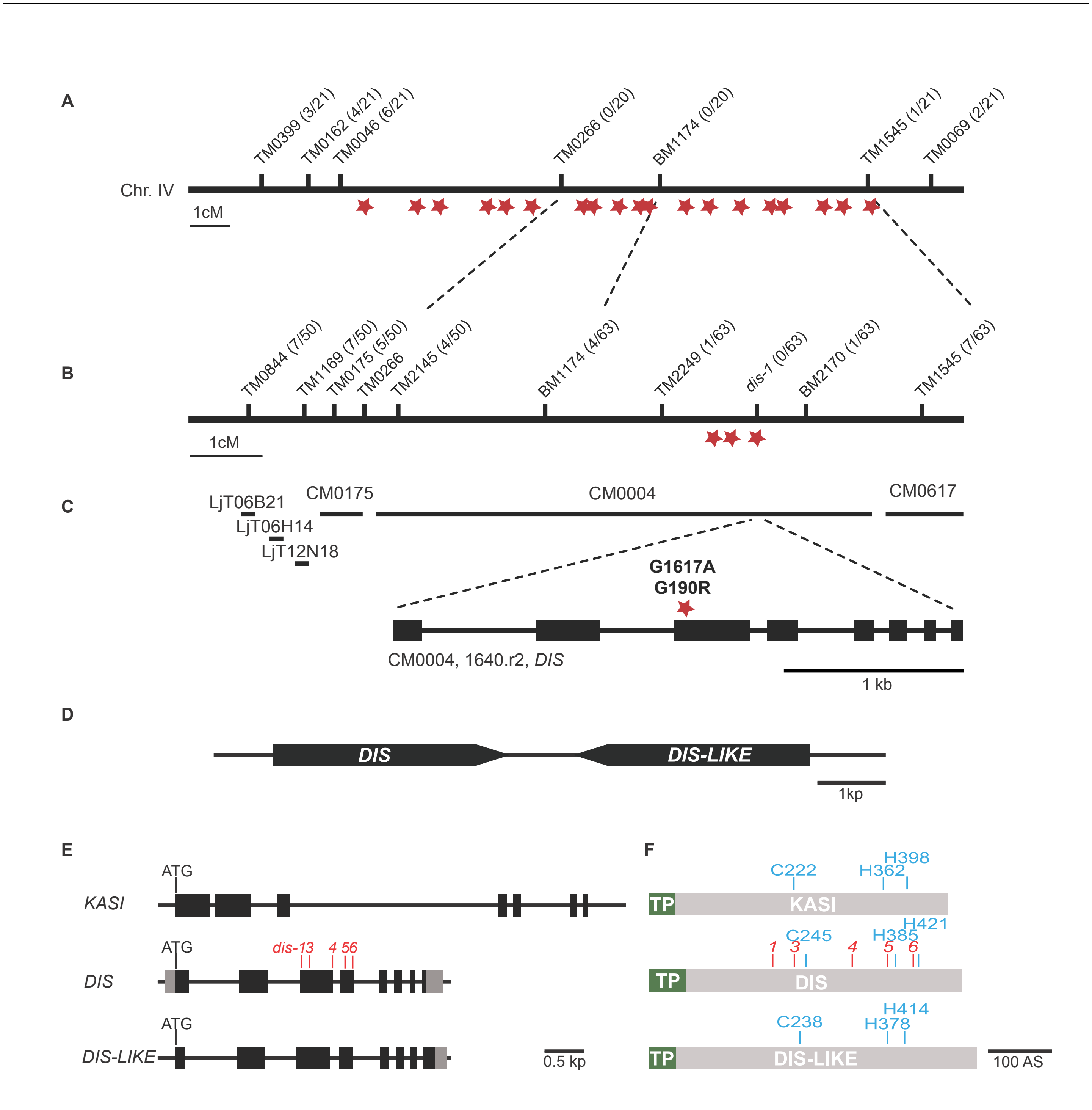

Figure 1—figure supplement 1. Identification of the *dis* mutation. (**A–B**) Genetic map of the *DIS* locus on chromosome 4. Numbers next to marker positions refer to the proportion of recombinant individuals among the number of analyzed F2 mutant plants. Rough mapping had previously identified the position of the *dis* mutation on the south arm of chromosome 4 (***Groth et al., 2013***). (**A**) In the first fine-mapping round, the interval narrowed down by recombinants comprised 19 EMS-induced SNPs (red stars), that could be confirmed by re-sequencing the mutant genome using next generation sequencing. (**B**) Further fine mapping resulted in an interval with 3 of these confirmed SNPs. (**C**) Physical map of the *DIS* locus. LjT followed by a number refers to TAC clones. CM followed by a number refers to contigs. One of the three SNPs causes a G to A transition in exon 3 of chr.4. CM004.1640.r2.a resulting in an amino acid change from glycine to arginine at position 190 of the protein product, which shares 79% sequence identity with a β-keto-acyl ACP synthase I (KASI) from *Arabidopsis thaliana*. Black boxes indicate exons separated by introns. (**D**) The *DIS* gene is duplicated in

Figure 1—figure supplement 1 continued on next page

Figure 1—figure supplement 1 continued

tandem. (**E**) Gene structure of *DIS*, *DIS-LIKE* and *KASI*. Black boxes display exons separated by introns (black lines). Grey boxes indicate determined untranslated regions. (**F**) DIS, DIS-LIKE and KASI are predicted to contain a plastid transit peptide (green). The catalytic triad is shown in blue and the location of mutations identified by TILLING in the *DIS* gene are shown in red. We chose the *dis-4* mutant for further analysis because the mutation resulted in a glycine replacement, which likely affects the functionality of the protein.
DOI: 10.7554/eLife.29107.004

A

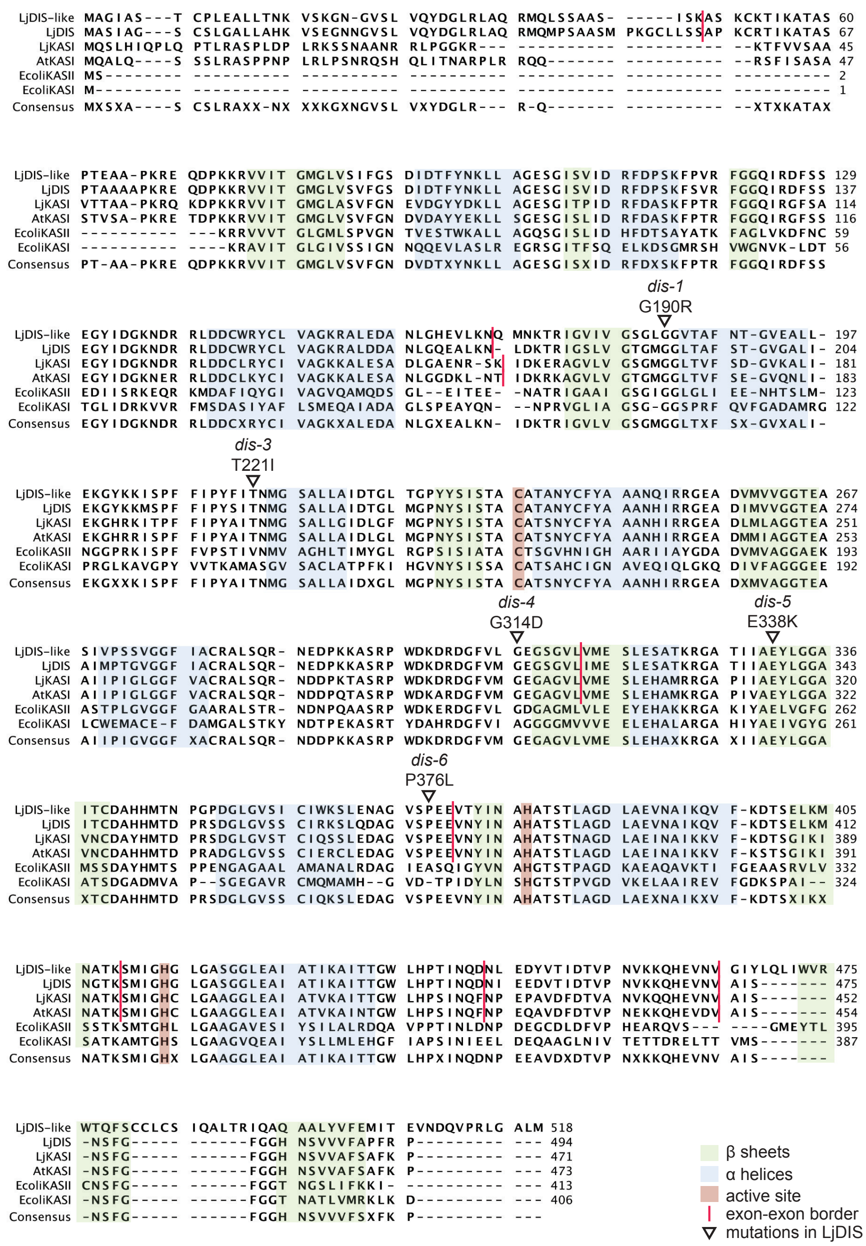

B

Percentage identity matrix:

	LjDIS	LjDIS-LIKE	LjKASI	AtKASI
LjDIS	100	87	79	78
LjDIS-LIKE	87	100	75	72
LjKASI	79	75	100	83
AtKASI	78	72	83	100

Figure 1—figure supplement 2. Protein sequence alignment of *L. japonicus* DIS with other KASI proteins. (**A**) Sequence alignment of LjDIS, LjDIS-LIKE, LjKASI, AtKASI and *E. coli* KASI and KASII. (**B**) Identity matrix of LjDIS, LjDIS-LIKE, LjKASI and AtKASI.

Figure 1—figure supplement 2 continued on next page

Figure 1—figure supplement 2 continued

DOI: 10.7554/eLife.29107.005

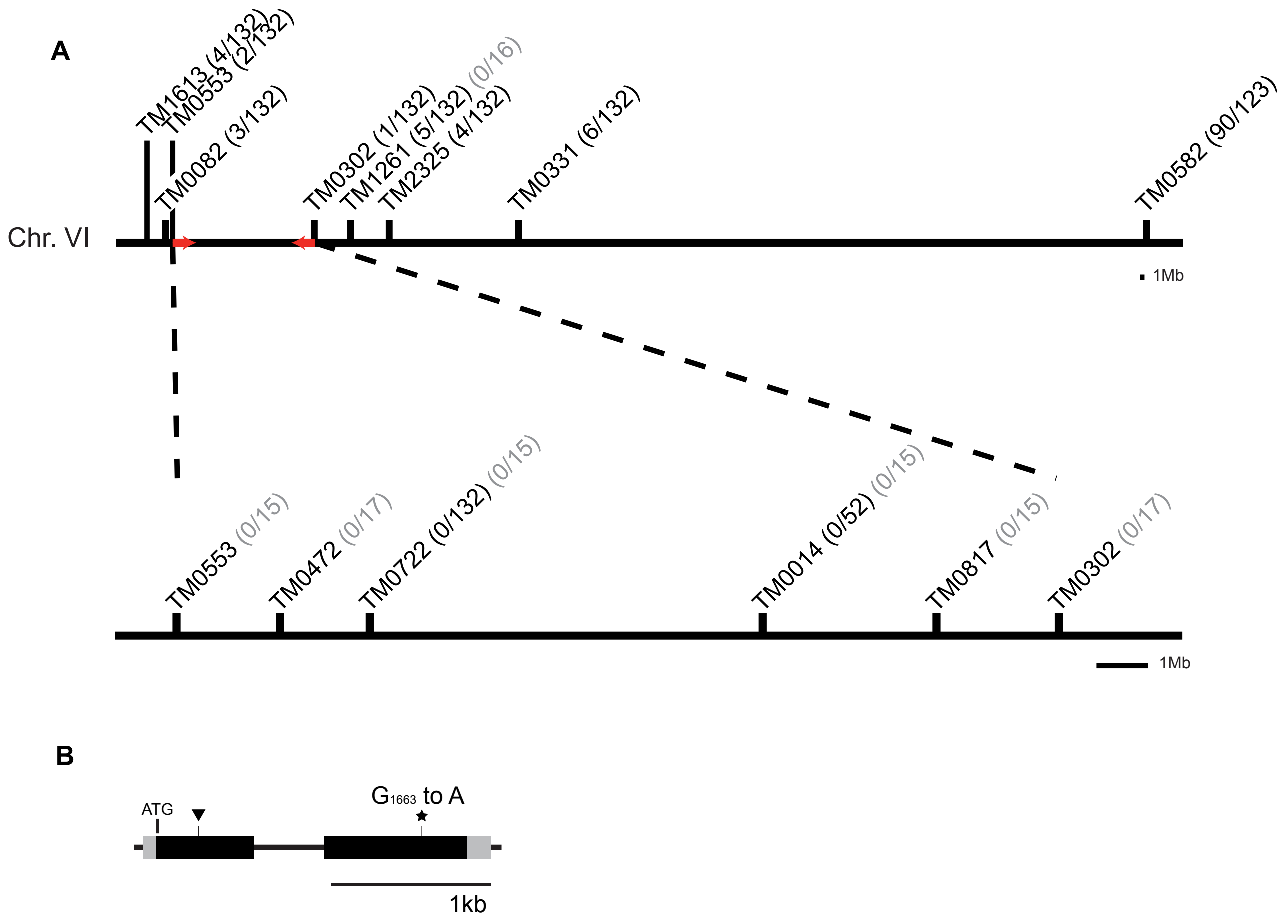

C

Generation	Phenotype	TM0553	TM0302	Nucleotide	No. of plants
F3	wild type	MG20	MG20	G	3
F3	wild type	Het	Het	R	8
F3	mutant	Gifu	Gifu	A	10
F4	wild type	Het	Het	R	4
F4	mutant	Gifu	Gifu	A	4

Figure 1—figure supplement 3. Identification of mutation in the *RAM2* gene. (**A**) Genetic map of the *red* locus on chromosome 6. Numbers next to the marker position refer to the proportion of recombinant individuals among the number of analysed F3 (black) and F4 (grey) segregating and mutant plants respectively. Fine mapping narrowed down the interval between TM0553 and TM0302. Red arrows indicate the genomic interval that contains the causative mutation. (**B**) Gene structure of *L. japonicus RAM2* with locations of the identified EMS-induced mutation at position 1663 (star, *ram2-1*) leading to an amino acid exchange from glycine to glutamic acid at position 555 of the RAM2 protein and LORE1 insertion (triangle, *ram2-2*). Black boxes indicate exons separated by intron (thin black line). Grey boxes indicate untranslated regions (UTRs) comprising 77 bp (5'UTR) and 151 bp (3'UTR). (**C**) Co-segregation analysis of arbuscule phenotype and mutation in the *RAM2* gene in a number of F3 and F4 plants from segregating populations containing only the mutation on chromosome 6. The number of plants analysed per generation, arbuscule phenotype, genotype at markers TM0053 and TM0302 and the nucleotide observed at position 1663 in the *RAM2* gene are indicated. The *ram2* mutation at position 1663 clearly co-segregates with the stunted arbuscule phenotype.

DOI: 10.7554/eLife.29107.006

A

```
                                                      Ljram2-2
                                                         ▽
LjRAM2           ---------- ---------- --MVSSTFPA VNKCT-SIGR EKHTVVADMD GTLLIGRSSF PYFALVAFEA 47
MtRAM2           MHPCLVETES VSLLQEEITI ITMASSTFPT VNKCT-SIGR EKHTVVADMD GTLLIGRSSF PYFALIAFEV 69
Lj1g3v2301880.1  ---------- ---------M VMGAFGHFKP ISKCS-TEER SNQTVASDFD GTLLVSPSAF PYYMLVAIEA 50
Medtr7g067380    ---------- ---------M VMGAFHHFKP ISKYNNSQDR SNQTIASDLD GTLLVSRDAF PYYMLMATEA 51
Consensus        ---------- ---------M VMXAXSXFXP XXKCT-SIGR XXXTVXXDMD GTLLXXRSXF PYXXLVAFEA

LjRAM2           GGILRLFFYL LCAPIAGILY YFVSEAAGIQ VLIFASMAGM KVSSIESVAR AVLPKFYSGD LHPESWRVFS 117
MtRAM2           GGVLRLLIYL LASPIAAILY YFISESAGIQ VLVFASMAGM KLSSIESVAR AVLPKFYSSD LHPETWRVFS 139
Lj1g3v2301880.1  GSYLRGLLLL ASVPFVYFTC LFISETAAVK TLIFITFAGL KIKDVEMVTA SVLPKFYAED VHPETWRVFN 120
Medtr7g067380    GSFLRGIILL ISVPFVYFTY LFVSETIAIK MLIFITFAGL KINDVEMVSR SVLSKFYAED VRPETWNVFN 121
Consensus        GXXLRXLIXL LSVPXXYXXY XFXSETAXIX VLIFXXXAGX KISXXEXVAR XVLPKFYXED XHPETWRVFX

LjRAM2           SCGKRCVLTA NPRIMVEPFL KEFLGADMVL GTEIGTYK-G RATGMICKPG ILVGGKKADA LKKAFGEEQP 186
MtRAM2           SCGKRCVLTA NPRIMVEPFL KEFLGADMVL GTEIASYK-G RATGLICKPG ILVGDKKAQV LKKTFGDEKP 208
Lj1g3v2301880.1  SFGKRCIVTT SPRLMVEPFA KSFLGADKVL GTELDATKSG RATGFAKEPG LLVGEHKKEA LVKEFQSNLP 190
Medtr7g067380    SFGKRYVVTA SPRLMVEPFV KNLLGGDRVI GTELEVTKSG RVTGFVKEPG VLVGELKKDA VVKEFQSNLP 191
Consensus        SXGKRCVXTA XPRXMVEPFL KEFLGADMVL GTEXXXXKSG RATGFIXXPG ILVGEKKXDA LXKEFXSXLP

LjRAM2           DIGLGDRLTD APFMALCK|EG YIVPPNPKVK AVTTDKLPKP IIFHDGRLVH KPTPLLALLI ILWIPIGFPL 256
MtRAM2           DIGLGDRVTD APFMALCK|EG YIVPAKPKVT TVTSDKLPKP IIFHDGRLVQ KPTPLMALLI ILWIPIGFPL 278
Lj1g3v2301880.1  DLGLGDSETD HDFMSICK|EA YIVP-RIKCE ALPRNKLLSQ VIFHEGRFAQ RPTPLAALLT FLWLPISIML 259
Medtr7g067380    DLGLGDSESD HDFMSLCK|EG YMVP-RIKCD PLPRTKLLSP IIFHEGRFVQ RPTPIVALLS FLWLPIGIIL 260
Consensus        DXGLGDXETD XXFMXLCKEG YIVP-RXKXX AXXRDKLXXP IIFHXGRXVQ XPTPLXALLI XLWXPIGXPL

LjRAM2           ACLRIAAGSL LPMKLVYHAF WALGVRVIVK GTPPPPVGKS NP-HKSGVLF ICSHRTLLDP IFLSTALGRP 325
MtRAM2           ACLRIAAGSL LPMKFVYCAF KALGVRVIVK GTPPPPVETS KTNHQSGVLF ICSHRTLLDP IFLSTALGRA 348
Lj1g3v2301880.1  SILRVYLNIP LPEKIAWYNY KLLGIRVTVK GTPPPPPKKG QK----GVLF VCNHRTVLDP VVTAVALGRK 325
Medtr7g067380    SILRVYLNIP LPEKIAWYNY KLLGIKVIVK GTPPPAPKKG QK----GVLF VCNHRTILDP VVTAVALGRK 326
Consensus        XXLRXXXXXX LPXKIXXYXX KXLGXRVIVK GTPPPPXKKX QK-H-SGVLF XCXHRTLLDP XXXXXALGRK

LjRAM2           IPAVTYSVSR LSEIISPIKT VRLSRDRATD ASMIKKLLQE GDLAICPEGT TCREPFLLRF SALFAELTDE 395
MtRAM2           IPAVTYSVSR LSEIISPIKT VRLSRDRATD AAMIKKLLQE GDLAICPEGT TCREPFLLRF SALFAELTDE 418
Lj1g3v2301880.1  ISCVTYSISK FSEIISPIKA VALSRDREKD AANIRRLLEE GDLVICPEGT TCREPFLLRF SALFAELTDR 395
Medtr7g067380    ISCVTYSISK FSEIISPIKA VALSREREKD AANIRKLLEE GDLVICPEGT TCREPFLLRF SALFAELTDR 396
Consensus        IXXVTYSXSX XSEIISPIKX VXLSRDRXXD AAXIXKLLXE GDLXICPEGT TCREPFLLRF SALFAELTDX

                      Ljram2-1
                         ★
LjRAM2           LVPVAMVNRM SMFHGTTARG WKGMDPFYFF MNPSPVYEVT FLNKLPKELT CTASKSSHDV ANYIQRVIAA 465
MtRAM2           LVPVAMVNRM SMFHGTTARG WKGMDPFYFF MNPSPVYEVT FLNKLPKELT CGSGKTSHEV ANYIQRVVAS 488
Lj1g3v2301880.1  IVPVAINTKQ SVFYGTTARG HKLLDPYFVF MNPMPTYEIT FLNQLPKELT CTGGKSAIEV ANYIQKVIAG 465
Medtr7g067380    IVPVAINTKQ SVFYGTTVRG HKVLDPYFVF MNPVPTYEIT FLNQLPKELT VSGGKSAIEV ANYIQRVLAG 466
Consensus        XVPVAXXXXX SXFXGTTARG XKGXDPXXXF MNPSPXYEXT FLNXLPKELT CTGGKSXXEV ANYIQRVIAG

LjRAM2           TLSYECTSFT RRDKYRALAG NDGTVAEKPK AANKVMGC 503
MtRAM2           TLSYECTSFT RRDKYRALAG NDGTVVEKTN KANKVMGC 526
Lj1g3v2301880.1  ALGFECTNLT RKDKYAMLAG TDGSVPSKKE KA------ 497
Medtr7g067380    TLGFECTNLT RKDKYAMLAG TDGRVPSKKE KA------ 498
Consensus        TLXXECTXXT RXDKYXXLAG XDGTVPXKKE KANKVMGC
```

| exon-exon border

★ G to E transition in *Ljram2-1*

▽ LORE1 insertion in *Ljram2-2*

B

Percentage identity matrix:

	LjRAM2	MtRAM2	Lj1g3v2301880.1	Medtr7g067380
LjRAM2	100	89.26	56.39	55.17
MtRAM2	89.26	100	56.45	55.44
Lj1g3v2301880.1	56.39	56.45	100	85.11
Medtr7g067380	55.17	55.44	85.11	100

Figure 1—figure supplement 4. Protein sequence alignment of *L. japonicus* RAM2 with *M. truncatula* RAM2. Sequence alignment (**A**) and identity matrix (**B**) of LjRAM2, Lj1g3v2301880.1, MtRAM2 and Medtr7g067380.

Figure 1—figure supplement 4 continued on next page

Figure 1—figure supplement 4 continued

DOI: 10.7554/eLife.29107.007

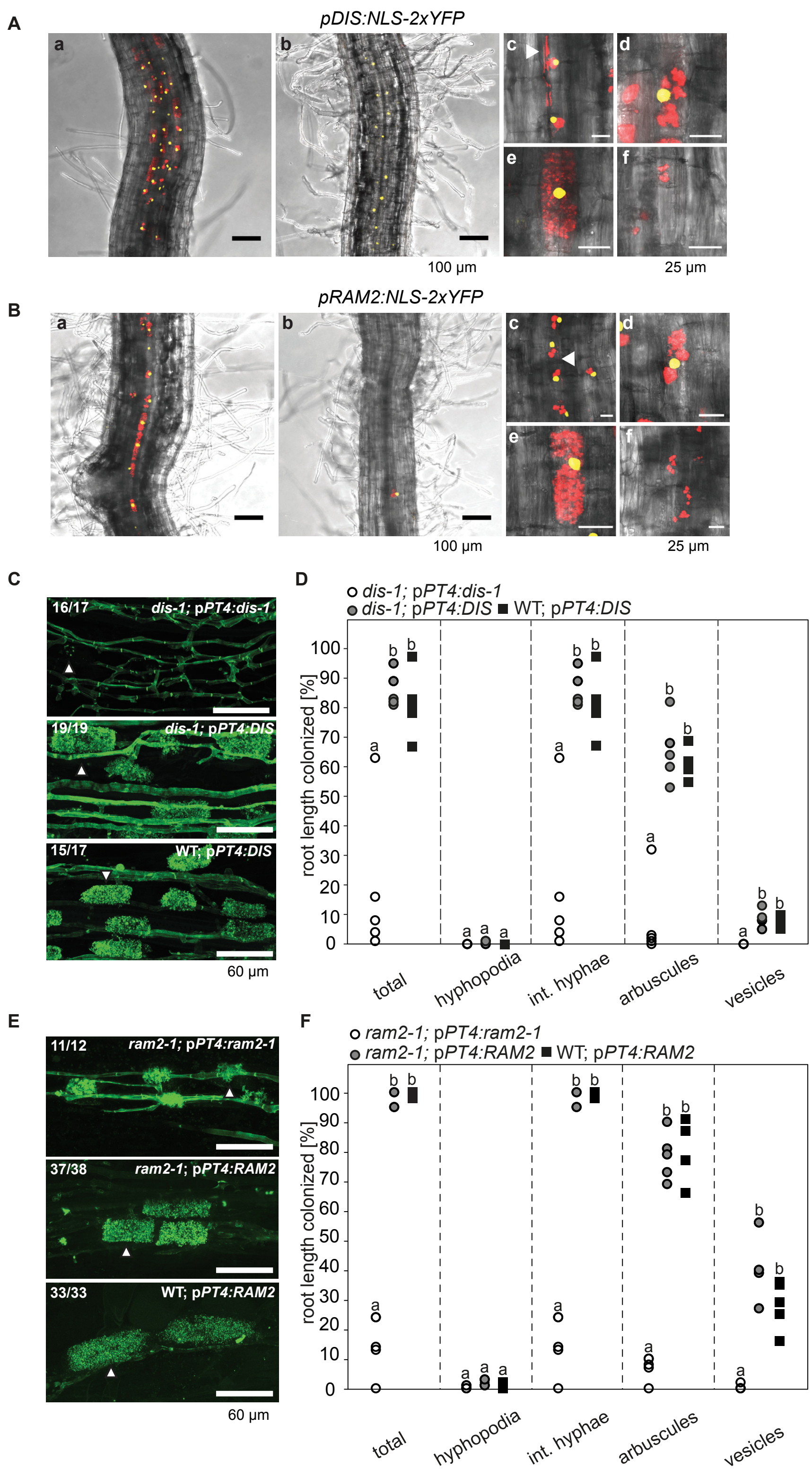

Figure 2. Arbuscocyte-specific expression of *DIS* and *RAM2* is sufficient for arbuscule branching. Promoter activity indicated by nuclear localized yellow fluorescence in colonized transgenic *L. japonicus* wild-type roots transformed with constructs containing a 1.5 kb promoter fragment of *DIS* (**A**) or a

Figure 2 continued on next page

Figure 2 continued

2.275 kb promoter fragment of *RAM2* (**B**) fused to *NLS-YFP*. (**A-B**) Red fluorescence resulting from expression of *pSbtM1:SP-mCherry* labels the apoplastic space surrounding pre-penetration *apparatuus* (PPAs) and fungal structures, thereby evidencing the silhouette of these structures. a Colonized root, b non-colonized part of colonized root, c PPAs, (white arrow heads indicate the silhouette of fungal intraradical hyphae) d small arbuscules, e fully developed arbuscules f collapsed arbuscules. Merged confocal and bright field images of whole mount roots are shown. (**C-D**) Transgenic complementation of *dis-1* (C) and *ram2-1* (D) hairy roots with the respective wild-type gene driven by the *PT4* promoter. The mutant gene was used as negative control. White arrowheads indicate arbuscules. (**E-F**) Quantification of AM colonization in transgenic roots shown in (**C-D**). Different letters indicate significant differences (ANOVA; posthoc Tukey; n = 15; $p \leq 0.001$) among genotypes for each fungal structure separately. Int. hyphae, intraradical hyphae. (**E**): $F_{2,12} = 26.53$ (total), $F_{2,12} = 46.97$ (arbuscules), $F_{2,12} = 27.42$ (vesicles). (**F**) $F_{2,12} = 341.5$ (total), $F_{2,12} = 146.3$ (arbuscules), $F_{2,12} = 35.86$ (vesicles).

DOI: 10.7554/eLife.29107.008

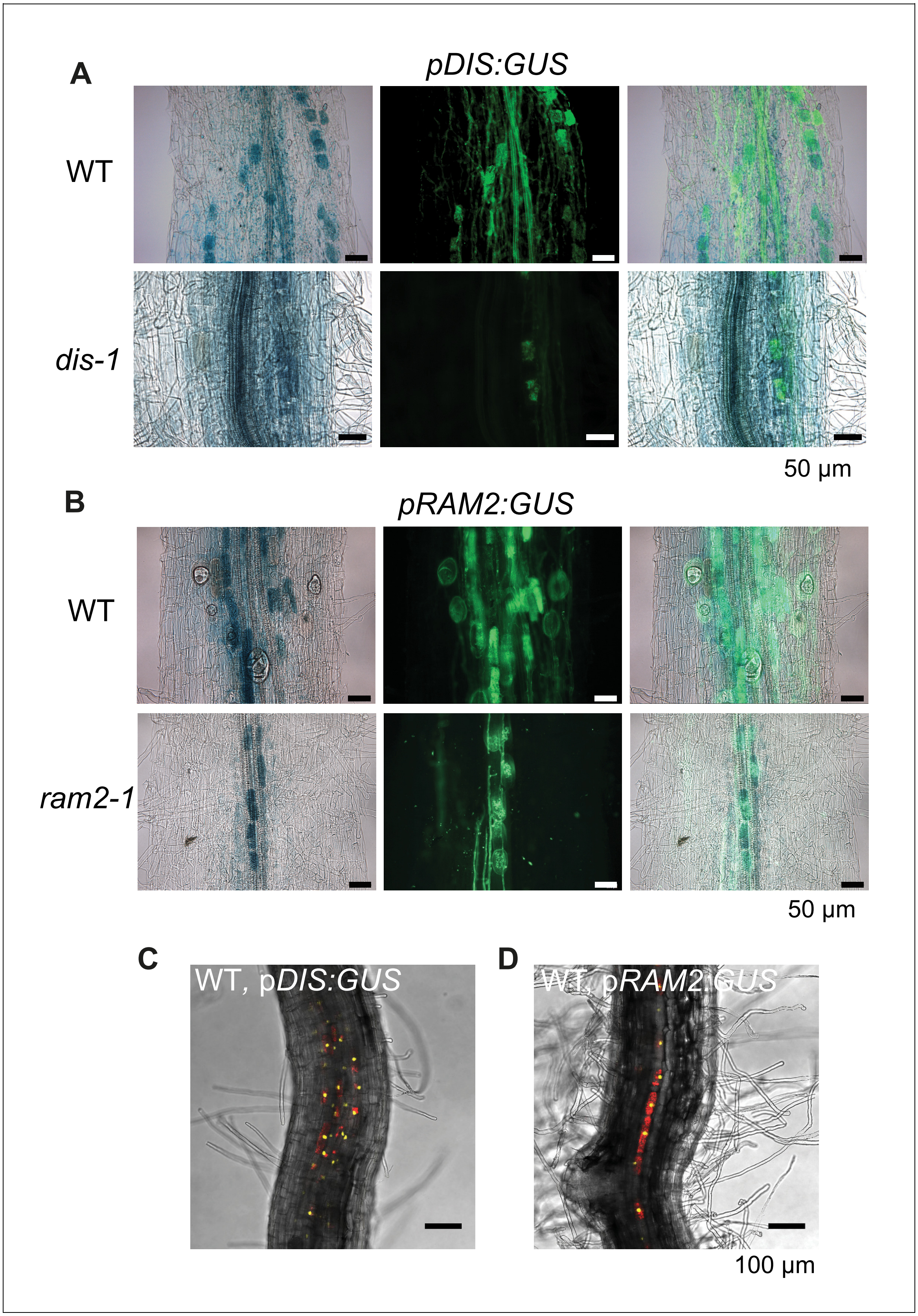

Figure 2—figure supplement 1. *DIS* and *RAM2* promoter activity in wild type and *dis* and *ram2* mutants. GUS activity in colonized transgenic *L. japonicus* wild-type and mutant roots transformed with constructs containing a 1.5 kb promoter fragment of *DIS* (**A**) or a 2.275 kb promoter fragment of

Figure 2—figure supplement 1 continued on next page

Figure 2—figure supplement 1 continued

RAM2 (**B**) fused to the *uidA* gene. Left micrographs: bright field channel to detect GUS-staining, middle micrographs: GFP-channel to detect (WGA)-AlexaFluor488 stained fungal structures. Right micrographs: Merge. (C-D) Single optical section of z-stack shown in ***Figure 2Aa*** (C) and ***Figure 2Ba*** (D) showing that *DIS* and *RAM2* promoter activity is detected exclusively in the cortex.
DOI: 10.7554/eLife.29107.009

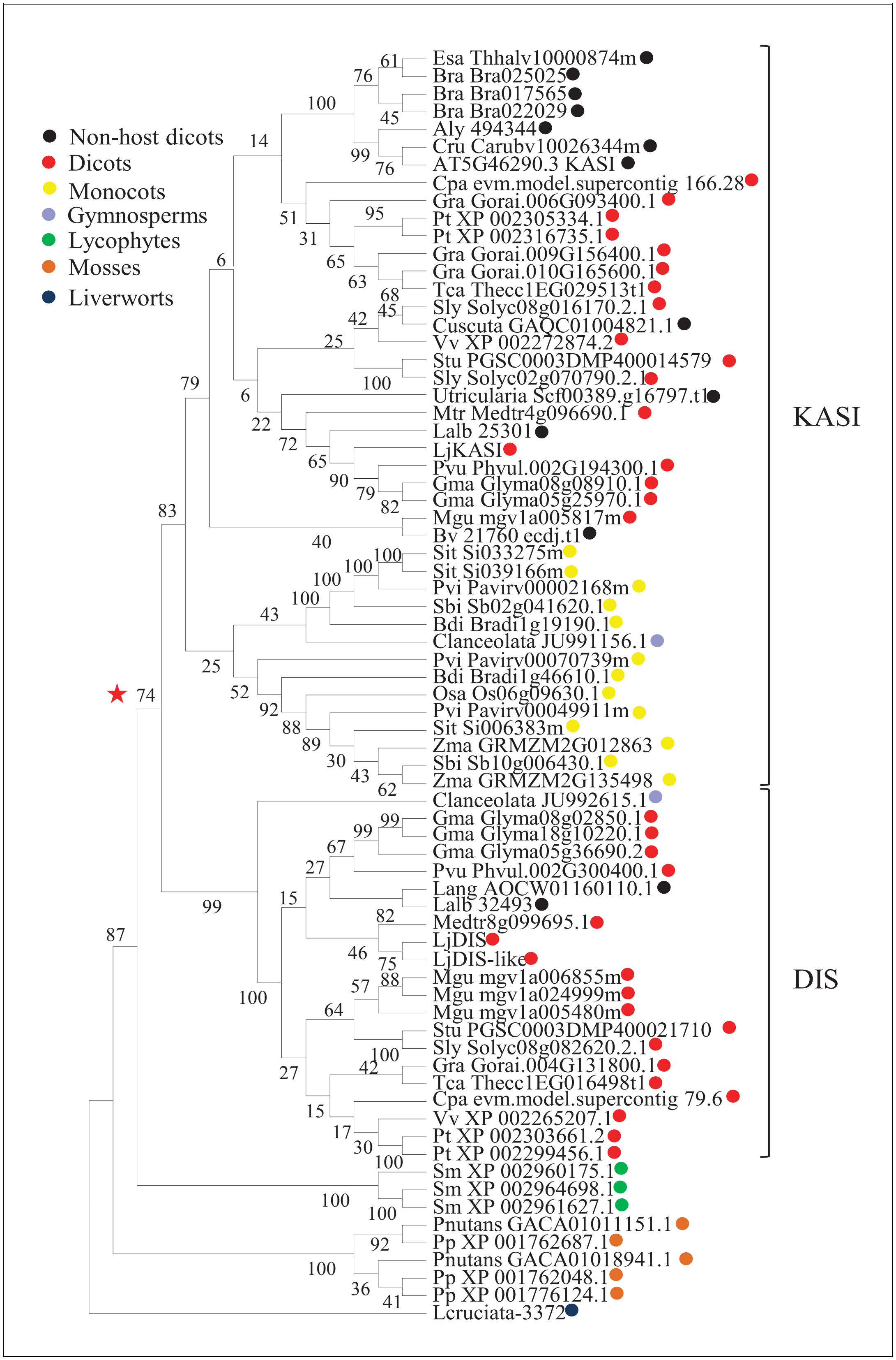

Figure 3. Phylogenetic tree of KASI proteins in land plants. Protein sequences were aligned using MAFFT. Phylogenetic trees were generated by neighbor-joining implemented in MEGA5 (***Tamura et al., 2011***). Partial gap

Figure 3 continued on next page

Figure 3 continued

deletion (95%) was used together with the JTT substitution model. Bootstrap values were calculated using 500 replicates. DIS likely originated before the angiosperm divergence (red star).

DOI: 10.7554/eLife.29107.016

The following source data is available for figure 3:

Source data 1. Accession numbers for protein sequences used in the phyologenic tree.

DOI: 10.7554/eLife.29107.017

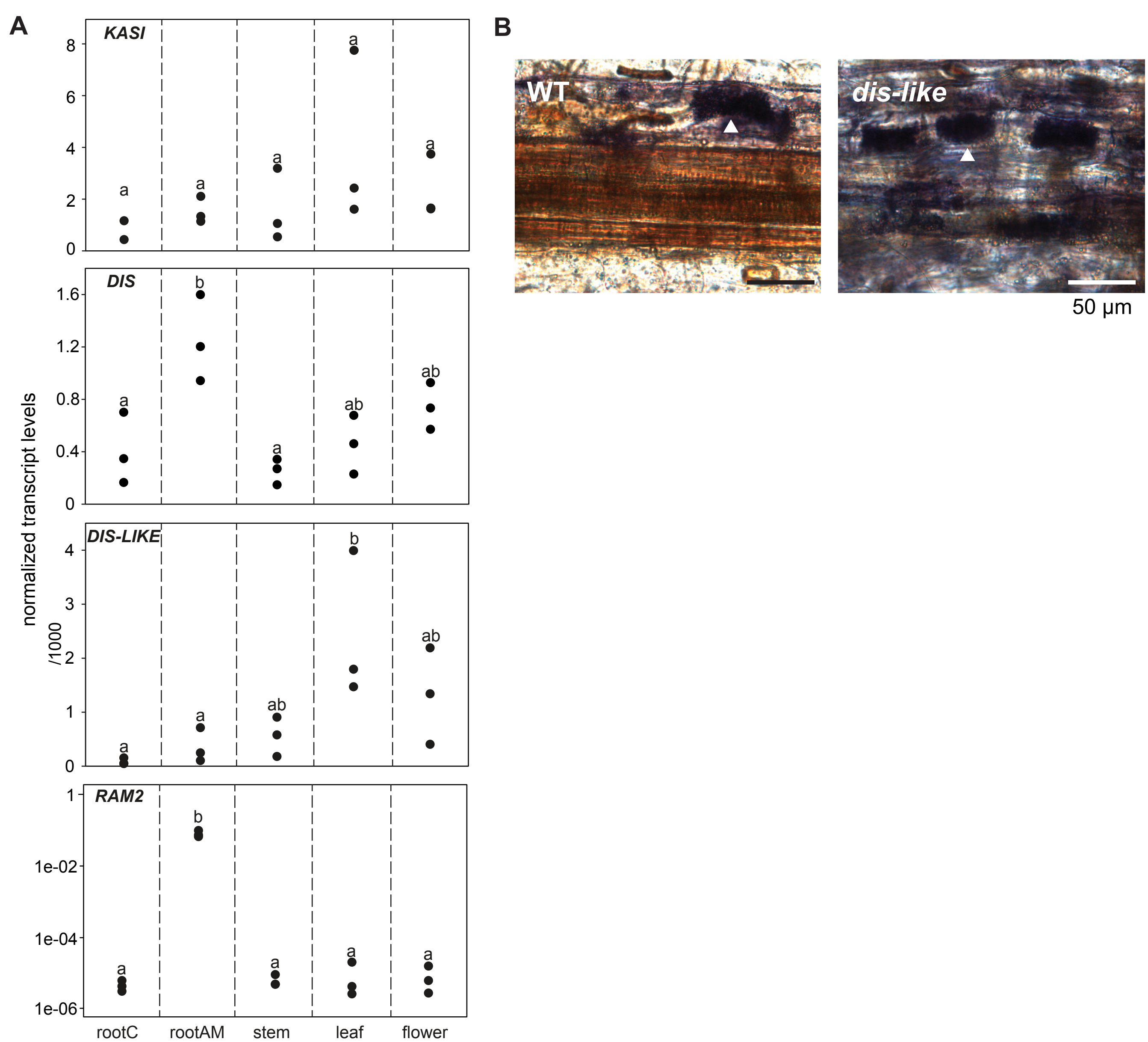

Figure 3—figure supplement 1. Transcript accumulation of *KASI* and *RAM2* genes. (**A**) Transcript accumulation of *DIS*, *DIS-LIKE*, *KASI* and *RAM2* in control (mock) and *R. irregularis* colonized (AM) roots and in different organs of *L. japonicus* assessed by qRT-PCR. Expression values were normalized to those of the constitutively expressed gene *EF1α* (*DIS*, *DIS-LIKE*, *KASI*) and *Ubiquitin10* (*RAM2*). Black circles represent three biological replicates. Different letters indicate significant differences (ANOVA; posthoc Tukey; n = 15; $p \leq 0.05$, $F_{4,14}$(*KASI*) = 1.191, $F_{4,14}$(*DIS*) = 8.412, $F_{4,14}$(*DIS-LIKE*) = 4.563; $p \leq 0.001$, $F_{4,14}$ = 67.41 (*RAM2*)). AM plants were inoculated with *R. irregularis*. Control and AM plants were harvested 5 wpi. (**B**) Arbuscule phenotype in wild type and *dis-like-5* mutant roots after 5 wpi with *R. irregularis* as indicated by acid ink staining. White arrow heads indicate arbuscules.

DOI: 10.7554/eLife.29107.018

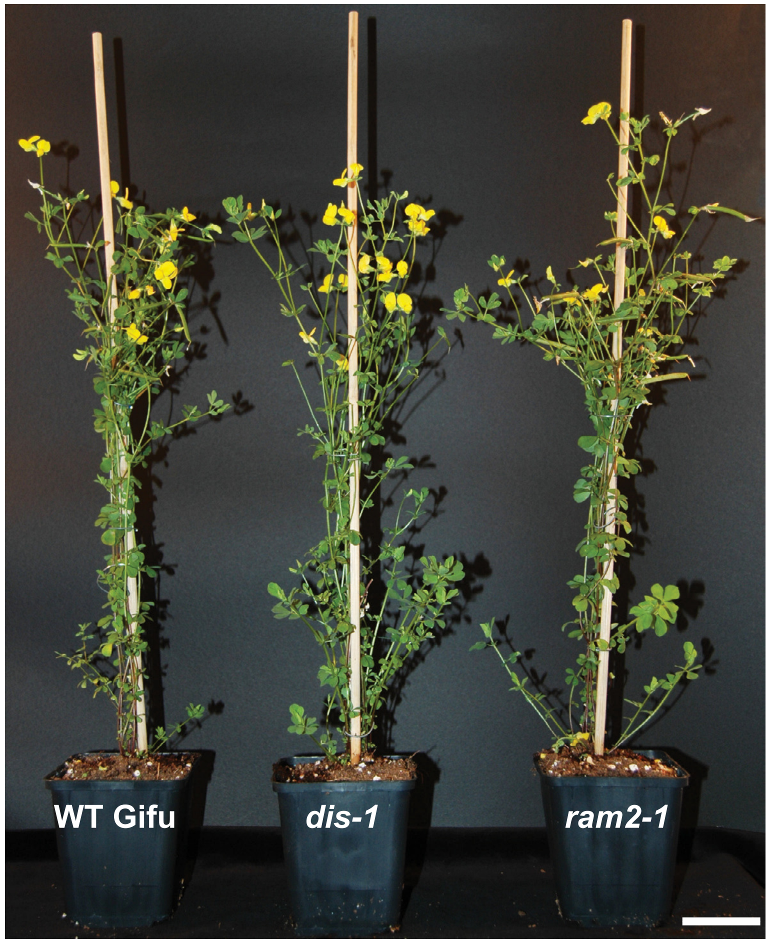

Figure 3—figure supplement 2. Shoot phenotypes of *dis* and *ram2* mutants. *dis* and *ram2* mutants do not show growth differences in shoot growth as compared to Gifu wild-type. The image has been taken 17 weeks post planting (size bar, 5 cm).

DOI: 10.7554/eLife.29107.019

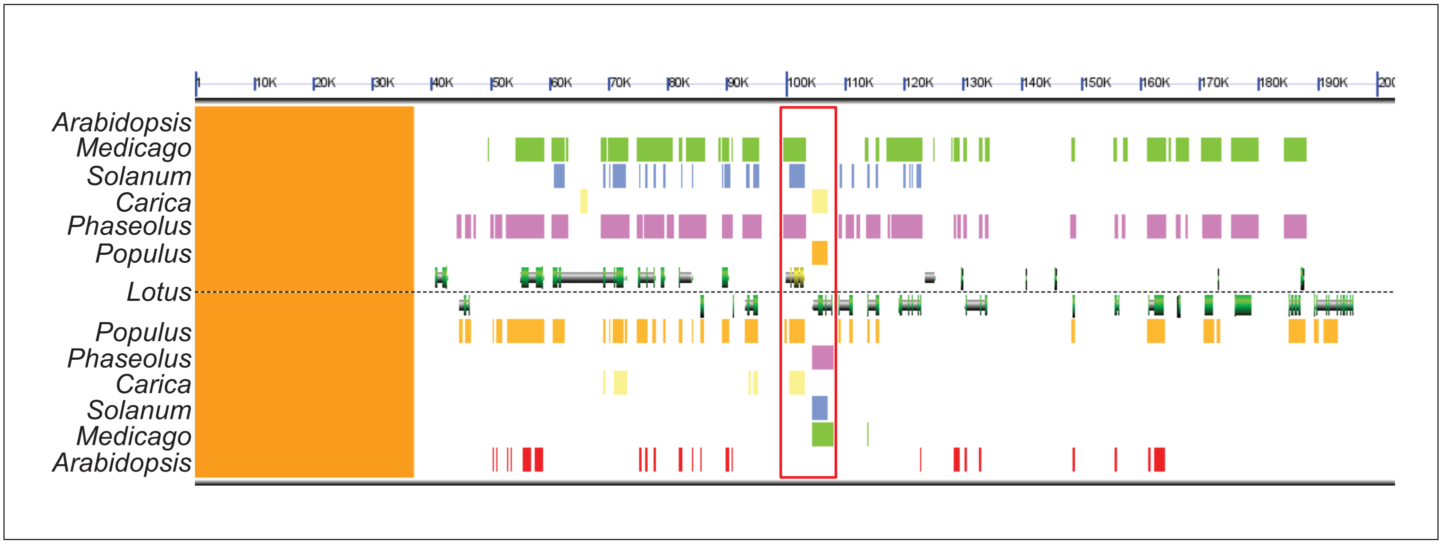

Figure 3—figure supplement 3. Genomic comparison of the *DIS* locus in host and non-host species. Synteny analysis of a ~ 200 kb sized region in the *Lotus japonicus*, *Medicago truncatula* (green), *Populus trichocarpa* (orange), *Phaseolus vulgaris* (pink), *Solanum lycopersicum* (blue) and *Carica papaya* (yellow) genomes containing the *DIS* locus. The genomic block is well conserved in these host species. By contrast, no *DIS* homolog was detected in the corresponding genomic block of *Arabidopsis thaliana* (red). The red rectangle indicates the *DIS* and *DIS-LIKE* locus, *DIS* is indicated in yellow. The sequences above *Lotus* correspond to the forward strand and those below *Lotus* to the reverse strand. The orange strip on the left side corresponds to a non-assembled region of the *L. japonicus* genome.

DOI: 10.7554/eLife.29107.020

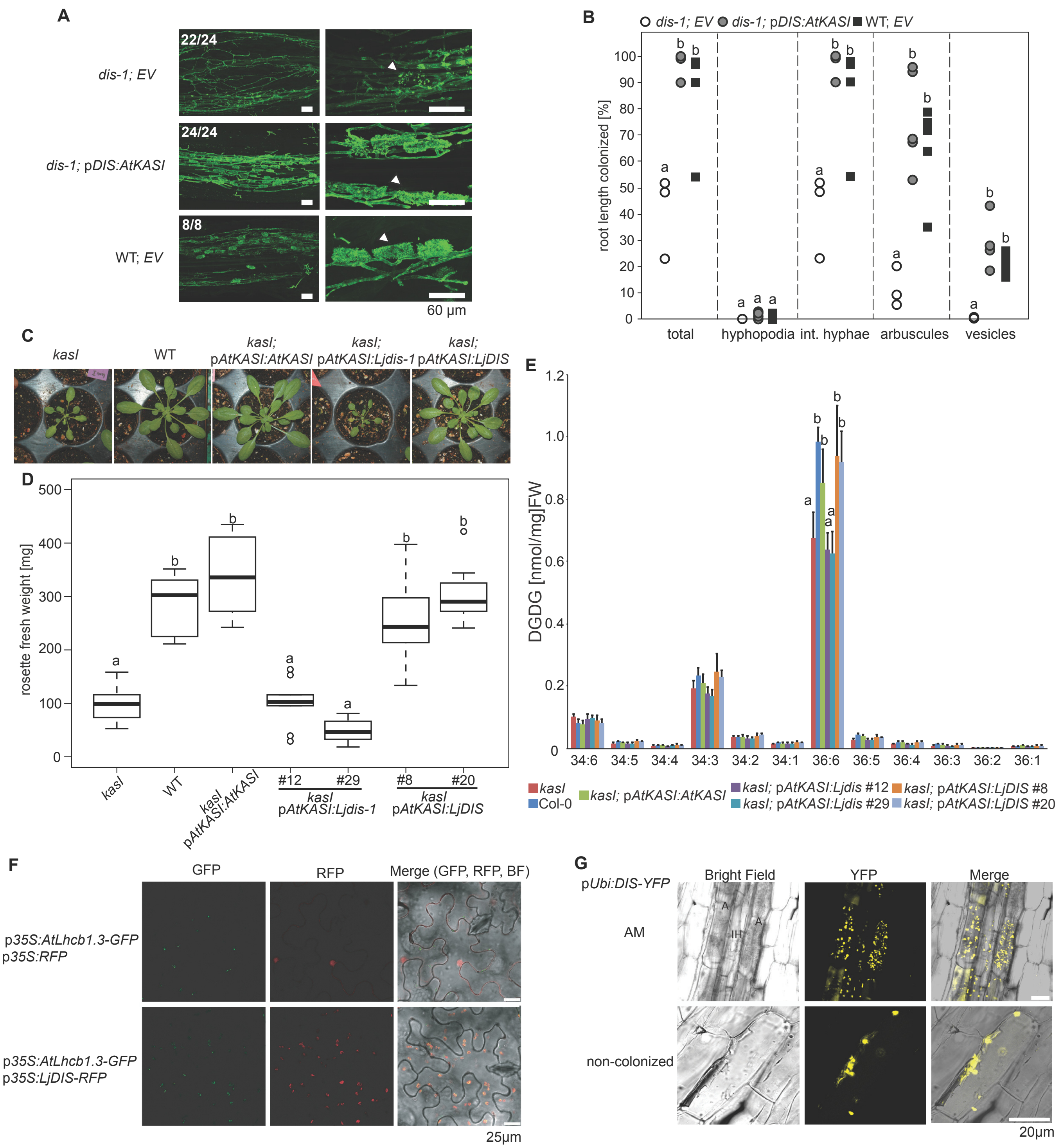

Figure 4. DIS function is equivalent to a canonical KASI. (A) Microscopic AM phenotype of transgenic *dis-1* mutant and wild-type hairy roots transformed with either an empty vector (EV) or the *Arabidopsis KASI* gene fused to the *L. japonicus DIS* promoter. White arrowheads indicate arbuscules. (B) Quantification of AM colonization in transgenic roots of *dis-1* transformed with EV (open circles), *dis-1* transformed with p*DIS-AtKASI* (grey circles) and wild-type transformed with EV (black squares). int. hyphae, intraradical hyphae. Different letters indicate significant differences (ANOVA; posthoc Tukey; n = 15; p≤0.001) among genotypes for each fungal structure separately. $F_{2,12}$ = 0.809 (total and intraradical hyphae), $F_{2,12}$ =

Figure 4 continued on next page

Figure 4 continued

43.65 (arbuscules), $F_{2,12}$ = 0.0568 (vesicles). (**C**) Rosettes of *Arabidopsis*, *kasI* mutant, Col-0 wild-type plants and *kasI* mutant plants transformed either with the native *AtKASI* gene, the *dis-1* mutant or the *DIS* wild-type gene driven by the *Arabidopsis KASI* promoter at 31 days post planting. (**D**) Rosette fresh weight of *kasI* mutant, Col-0 wild-type plants, one transgenic *pAtKASI:AtKASI* complementation line (***Wu and Xue, 2010***) and two independent transgenic lines each of *kasI* mutant plants transformed either with the *dis-1* mutant or the *DIS* wild-type gene driven by the *Arabidopsis KASI* promoter at 31 days post planting. Different letters indicate significant differences (ANOVA; posthoc Tukey; n = 70; $p \leq 0.001$; $F_{6,63}$ = 34.06) among genotypes. (**E**) Q-TOF MS/MS analysis of absolute amount of digalactosyldiacylglycerols (DGDG) containing acyl chains of 16:x + 18:x(34:x DGDG) or di18:x(36:x DGDG) derived from total leaf lipids of the different *Arabidopsis* lines. Different letters indicate significant differences (ANOVA; posthoc Tukey; n = 32; ($p \leq 0.05$, $F_{6,25}$ = 14.48 (36:6)). (**F**) Subcellular localization of DIS in transiently transformed *Nicotiana benthamiana* leaves. Free RFP localizes to the nucleus and cytoplasm (upper panel). RFP fused to DIS co-localizes with the *Arabidopsis* light harvesting complex protein AtLHCB1.3-GFP in chloroplasts (lower panel). (**G**) Subcellular localization in plastids of DIS-YFP expressed under the control of the *L. japonicus Ubiquitin* promoter in *R. irregularis* colonized (upper panel) and non-colonized (lower panel) *L. japonicus* root cortex cells. BF, bright field; IH, intercellular hypha; A, arbuscule.

DOI: 10.7554/eLife.29107.021

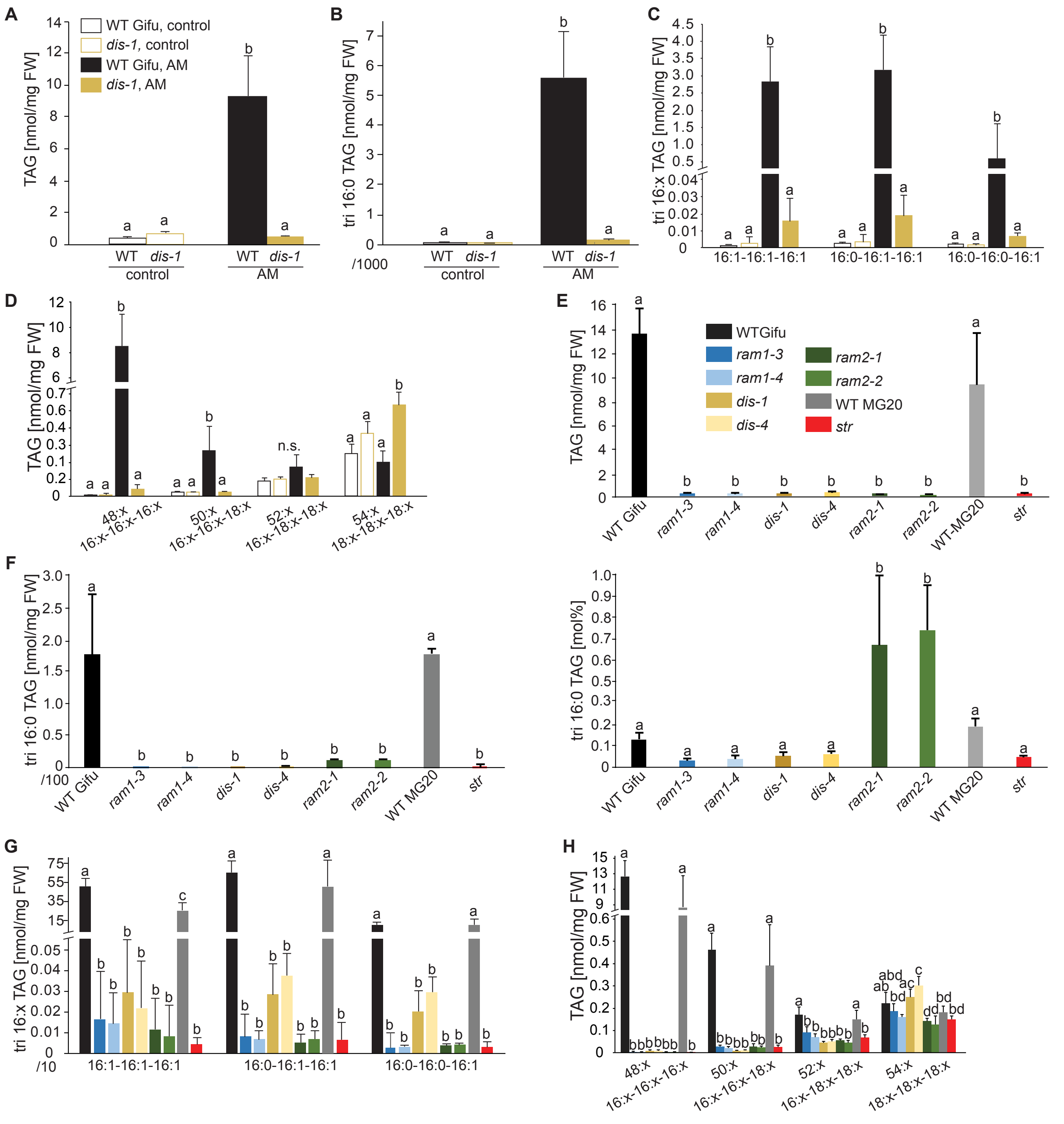

Figure 5. Lack of characteristic accumulation of triacylglycerols in AM-defective mutants. (**A-D**) Quantitative accumulation of (**A**) total triacylglycerols, (**B**) tri16:0-triacylglycerol (**C**) tri16:x-triacylglycerols and (**D**) of triacylglycerols harbouring 16:x and 18:x FA-chains in non-colonized and *R. irregularis* colonized wild-type and *dis-1* roots. Different letters indicate significant differences (ANOVA; posthoc Tukey) (**A**): n = 18; $p \leq 0.001$; $F_{3,14} = 68.16$. (**B**): n = 18; $p \leq 0.001$; $F_{3,14} = 68.48$. (**C**): n = 19; $p \leq 0.01$, $F_{3,15} = 7.851$ (16:1-16:1-16:1); $p \leq 0.001$, $F_{3,15} = 14.52$ (16:0-16:1-16:1); $p \leq 0.001$, $F_{3,15} = 39.22$ (16:0-16:0-16:1). (**D**): n = 19; $p \leq 0.001$, $F_{3,15} = 12.15$ (48:x), $F_{3,15} = 15.56$ (50:x); $p \leq 0.01$, $F_{3,15} = 22.93$ (54:x). (**E-G**) Quantitative accumulation of (**E**) total triacylglycerols, (**F**) tri16:0-triacylglycerols, (**G**) tri16:x-triacylglycerols and (**H**) of triacylglycerols harbouring 16:x and 18:x FA-chains in colonized roots of

Figure 5 continued on next page

Figure 5 continued

L. japonicus wild-type Gifu, wild-type MG-20 and arbuscule-defective mutants. Different letters indicate significant differences (ANOVA; posthoc Tukey). (**E**): n = 40; $p \leq 0.001$; $F_{8,31} = 38.42$. (**F**) Left: absolute tri16:0 TAG content: n = 40; $p \leq 0.001$; $F_{8,31} = 19.05$. Right: tri16:0 TAG proportion among all TAGs, n = 40; $p \leq 0.001$; $F_{8,31} = 14.21$. (**G**): $p \leq 0.001$; n = 41, $F_{8,32} = 86.16$ (16:1-16:1-16:1); n = 39, $F_{8,30} = 24.16$ (16:0-16:1-16:1); n = 40, $F_{8,31} = 17.67$ (16:0-16:0-16:1). (**H**): n = 40; $p \leq 0.001$, $F_{8,31} = 39.26$ (48:x), $F_{8,31} = 28.93$ (50:x); $p \leq 0.01$, $F_{8,31} = 19.78$ (52:x); $p \leq 0.05$, $F_{8,31} = 13.77$ (54:x). (**A-H**) Bars represent means ±standard deviation (SD) of 3–5 biological replicates.

DOI: 10.7554/eLife.29107.022

The following source data is available for figure 5:

Source data 1. Raw data for lipid profiles in ***Figure 5*** and ***Figure 5—figure supplements 1–3*** and ***5–11***.

DOI: 10.7554/eLife.29107.023

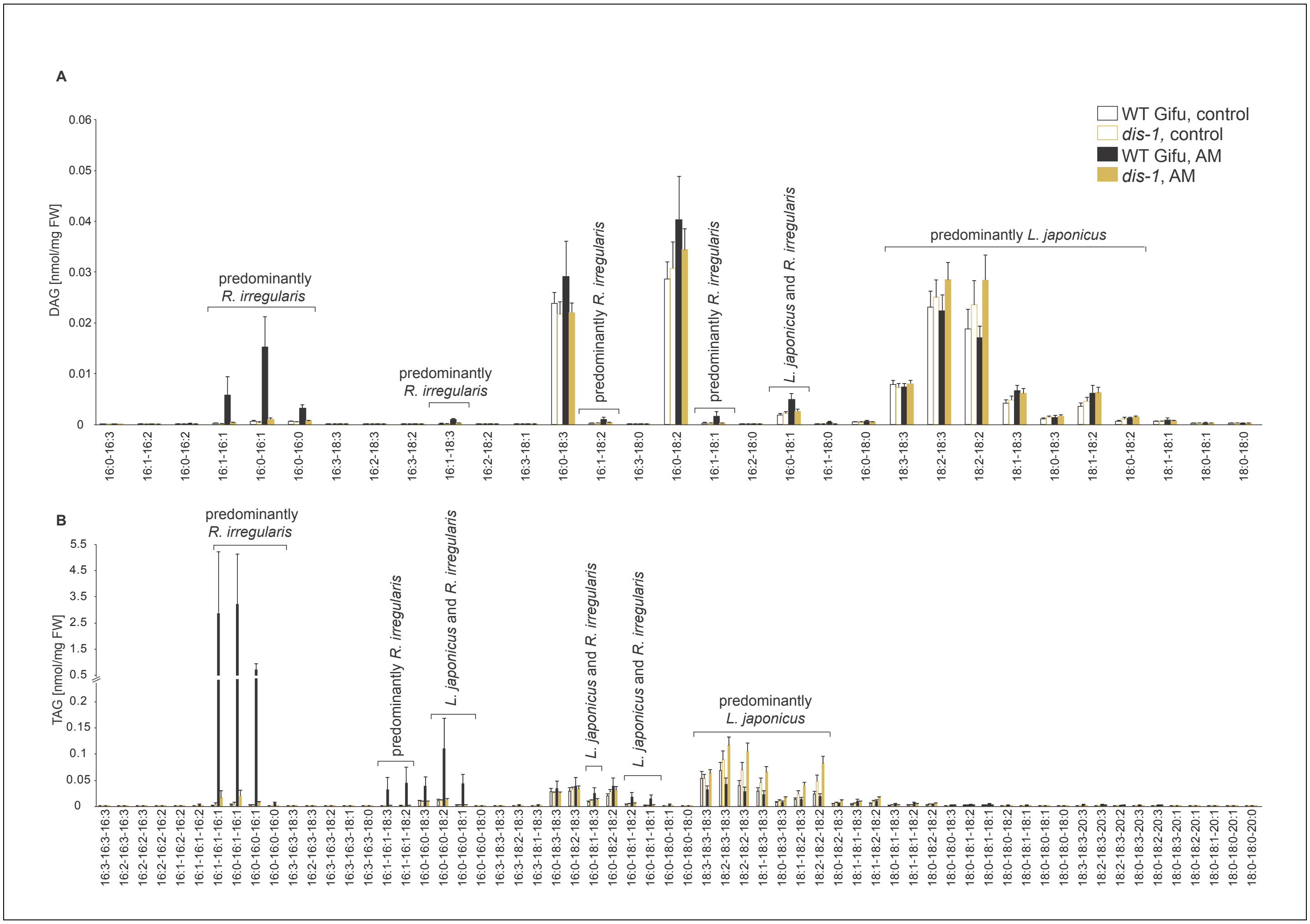

Figure 5—figure supplement 1. Diacylglycerol (DAG) and triacylglycerol (TAG) profiles of *L. japonicus* WT and *dis-1* control and AM roots. (**A**) Profile of diacylglycerols in control and AM-colonized *L. japonicus* WT and *dis-1* roots. (**B**) Profile of triacylglycerols in control and AM-colonized *L. japonicus* WT and *dis-1* roots. (**A–B**) Bars represent means ±standard deviation (SD) of 3–5 biological replicates. '*L. japonicus* and *R. irregularis*' marks lipids which are found in both organisms according to (***Wewer et al., 2014***) .

DOI: 10.7554/eLife.29107.024

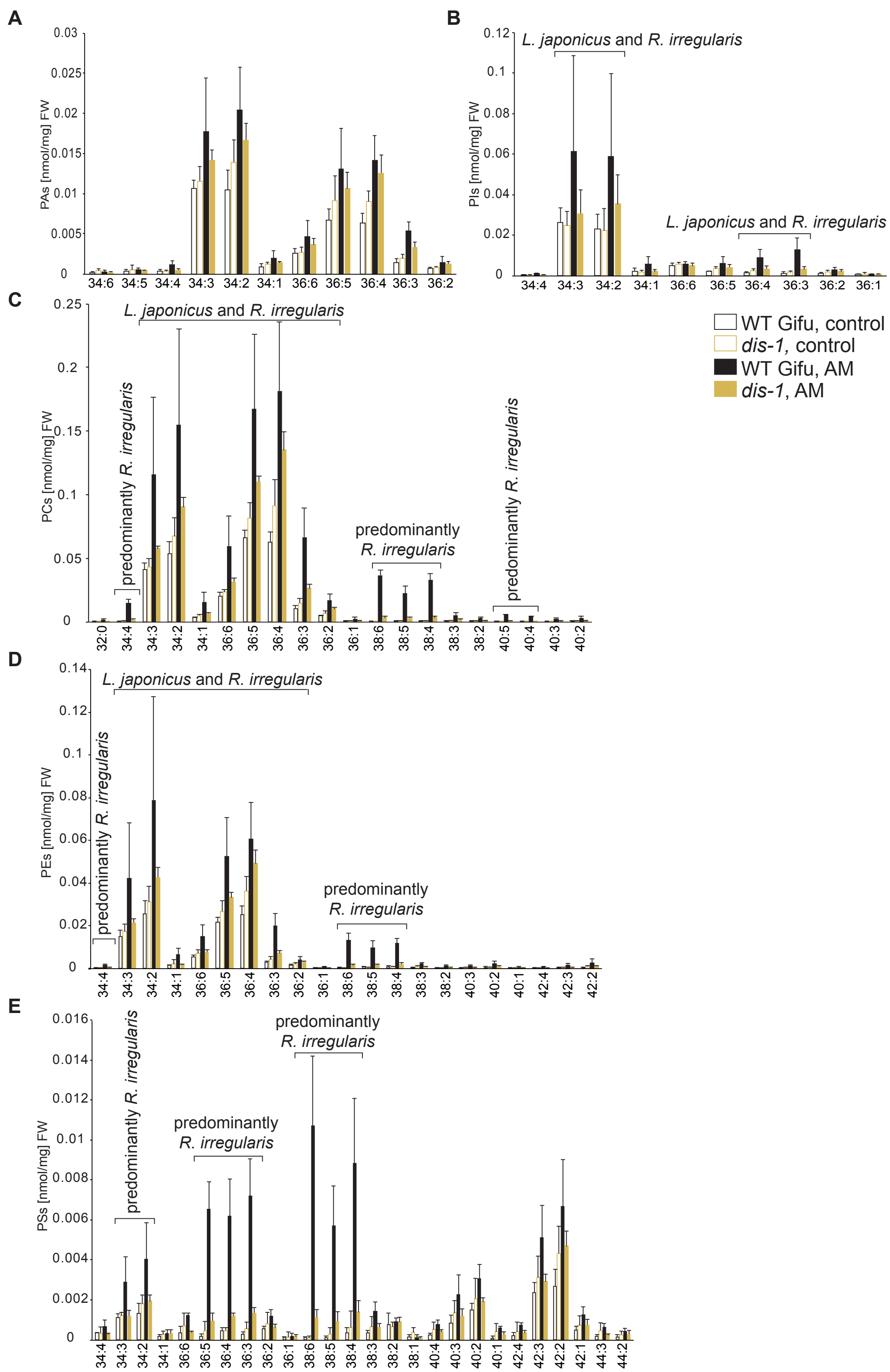

Figure 5—figure supplement 2. Profiles of phospholipids in non-colonized and colonized *L. japonicus* WT Gifu and *dis-1* roots. (**A**) Absolute amounts of phosphatidic acid (PA) species. (**B**) Absolute amounts of phosphatidylinositol (PI) species. (**C**) Absolute amounts of phosphatidylcholine (PC) species.

Figure 5—figure supplement 2 continued on next page

Figure 5—figure supplement 2 continued

(**D**) Absolute amounts of phosphatidylethanolamine (PE) species. (**E**) Absolute amounts of phosphatidylserine (PS) species. (**A–D**) Bars represent means ±standard deviation (SD) of 3–5 biological replicates. '*L. japonicus* and *R. irregularis*' marks lipids which are found in both organisms according to ***Wewer et al. (2014)***.

DOI: 10.7554/eLife.29107.025

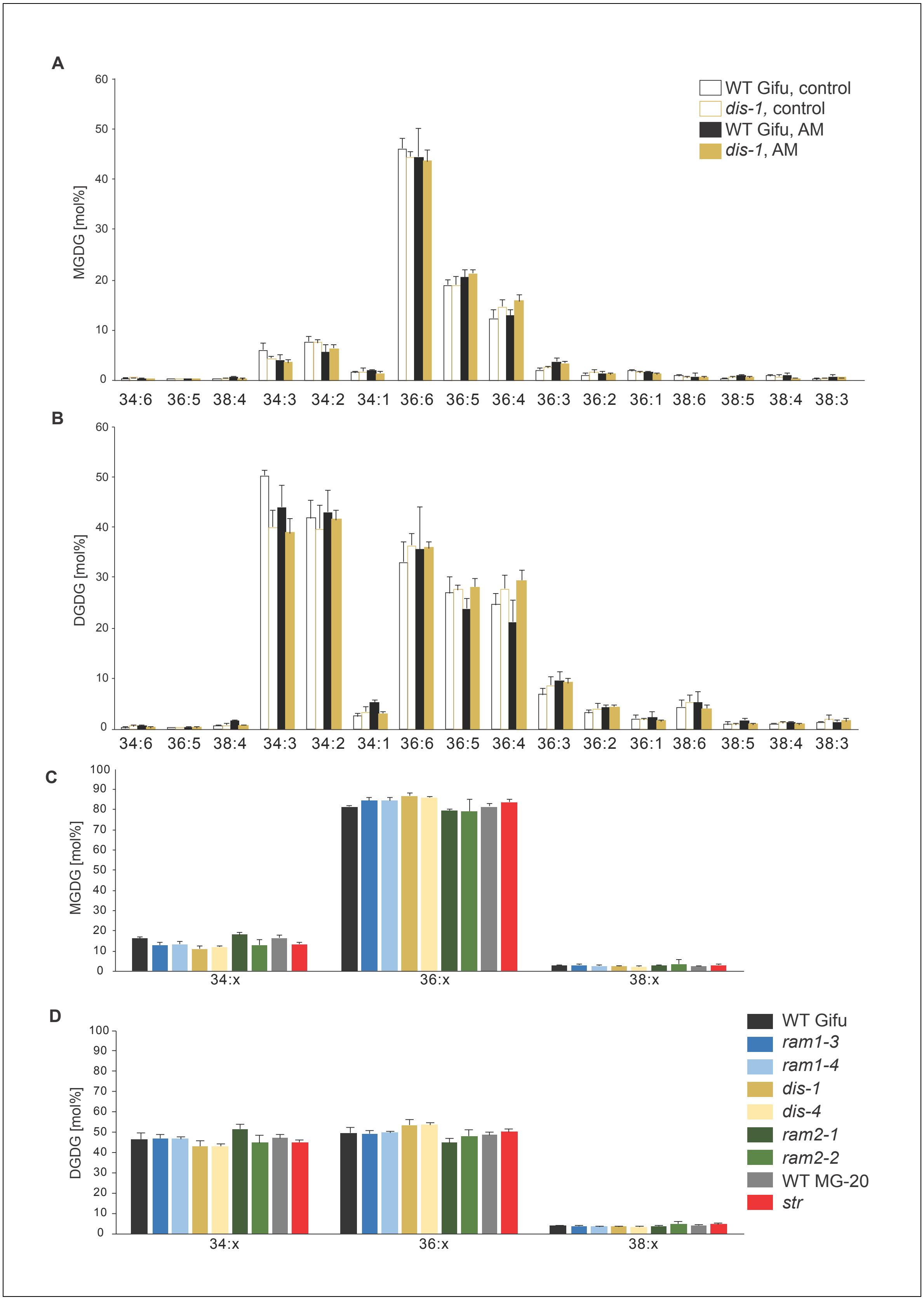

Figure 5—figure supplement 3. MGDG and DGDG profiles do not differ among *L. japonicus* wild-type and mutant roots. (**A**) Relative amounts of monogalactosyldiacylglycerol (MGDG) in control and colonized roots of Gifu WT and *dis-1*. (**B**) Relative amount of digalactosyldiacylglycerol (DGDG) in

Figure 5—figure supplement 3 continued on next page

Figure 5—figure supplement 3 continued

control and colonized roots of Gifu WT and *dis-1*. (**C**) Relative amounts of monogalactosyldiacylglycerols (MGDG) containing acyl chains of 16:x + 18:x (34:x MGDG), di18:x(36:x MGDG) or 18:x + 20:x(38:x MGDG) in the different colonized genotypes. (**D**) Relative amount of digalactosyldiacylglycerols (DGDG) containing acyl chains of 16:x + 18:x(34:x DGDG), di18:x(36:x DGDG) or 18:x + 20:x(38:x DGDG) of the different colonized genotypes. (**A–D**) Bars represent means ±standard deviation (SD) of 3–5 biological replicates.

DOI: 10.7554/eLife.29107.026

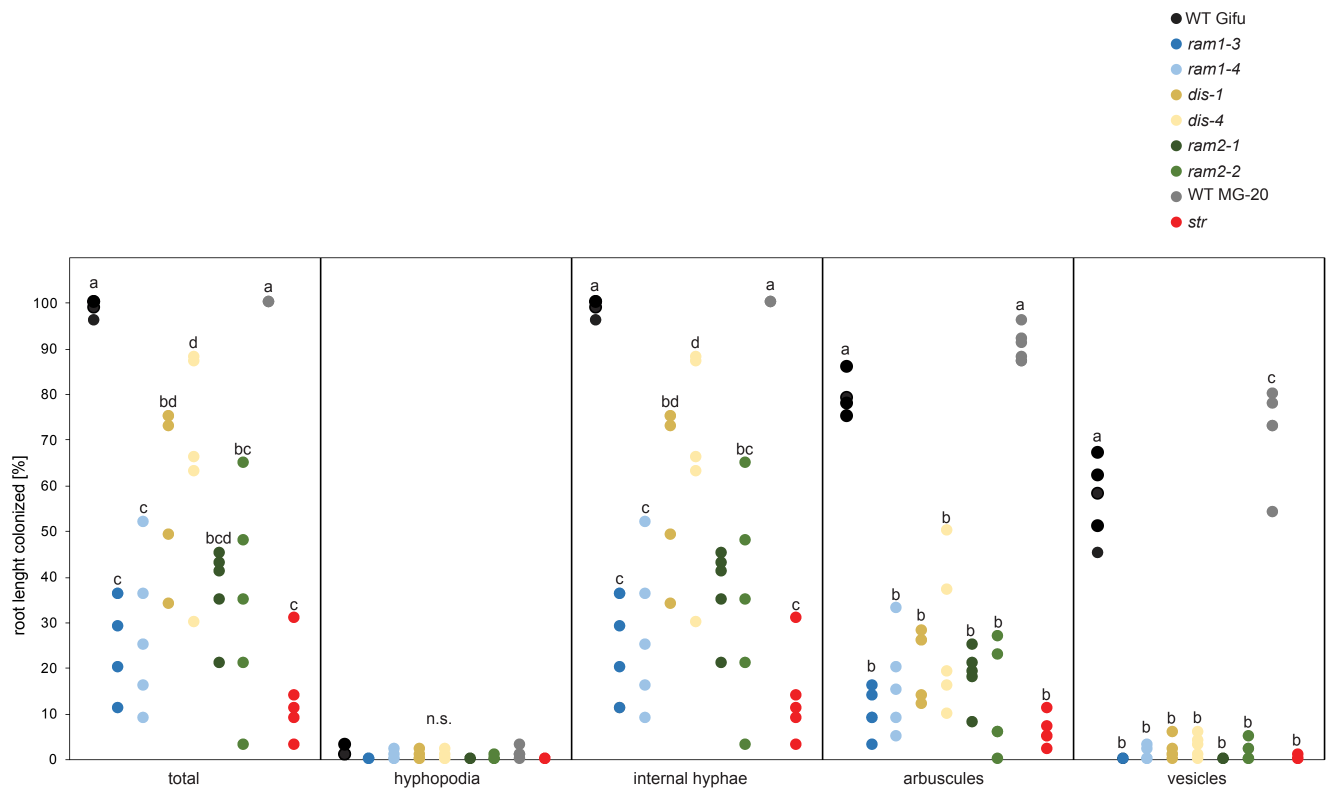

Figure 5—figure supplement 4. All arbuscule-deficient mutants show reduced root length colonization. Quantitative AM colonization in root samples employed for lipidomics (*Figure 3D–F*, *Figure 5E–H*, *Figure 7*, *Figure 5—figure supplements 1–3* and *5–11*) as determined by modified grid-line intersect methods after acid-ink staining. WT Gifu, WT MG-20 and all AM-deficient mutants in the Gifu background (*ram1-3, ram1-4, dis-1, dis-4, ram2-1* and *ram2-2)* and the *str* mutant in the MG-20 background. Different letters indicate significant differences (ANOVA; posthoc Tukey; n = 45) among genotypes for each fungal structure separately. $p \leq 0.05$, $F_{8,36} = 21.69$ (total and intraradical hyphae); $p \leq 0.001$, $F_{8,36} = 62.1$ (arbuscules), $F_{8,36} = 176.5$ (vesicles).

DOI: 10.7554/eLife.29107.027

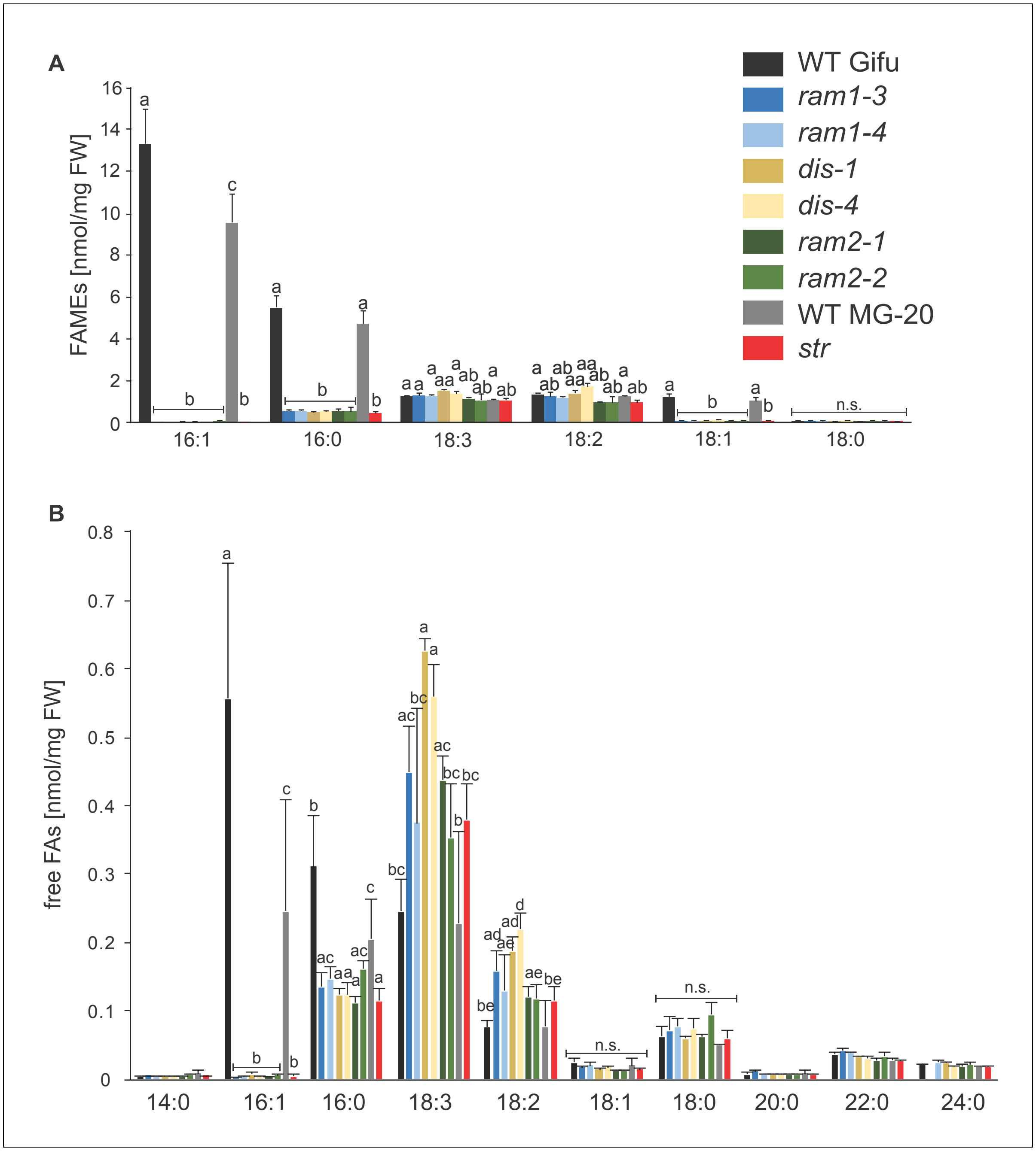

Figure 5—figure supplement 5. Total fatty acid and free fatty acid profiles of colonized *L. japonicus* WT and AM-defective mutant roots. (**A**) Total amounts of fatty acids (FAME) in colonized *L. japonicus* roots of the different genotypes. Fatty acid methyl esters (FAME) were prepared from total root lipids and analysed by GC. Different letters indicate significant differences (ANOVA; posthoc Tukey; $p \leq 0.01$; (n = 42, $F_{8,33}$ = 29.91 (16:1); n = 43, $F_{8,34}$ = 20.25 (16:0); n = 43, $F_{8,34}$ = 11.34 (18:3); $F_{8,34}$ = 13.14 (18:2)). (**B**) Free fatty acid composition in colonized *L. japonicus* roots from Gifu WT, MG-20 WT, *ram1-3, ram1-4, dis-1, dis-4, ram2-1, ram2-2* and *str*. Free fatty acids were isolated from total root lipids and converted into fatty acid methyl esters for quantification by GC Different letters indicate significant differences (ANOVA; posthoc Tukey; n = 44; ($p \leq 0.001$, $F_{8,35}$ = 230.6 (16:0); $p \leq 0.001$, $F_{8,35}$ = 257.7 (16:1); $F_{8,35}$ = 222.5 (18:1); $F_{8,35}$ = 15.48 (18:2); $F_{8,35}$ = 8.225 (18:3)). (**A–B**) Bars represent means ±standard deviation (SD) of 3–5 biological replicates.

DOI: 10.7554/eLife.29107.028

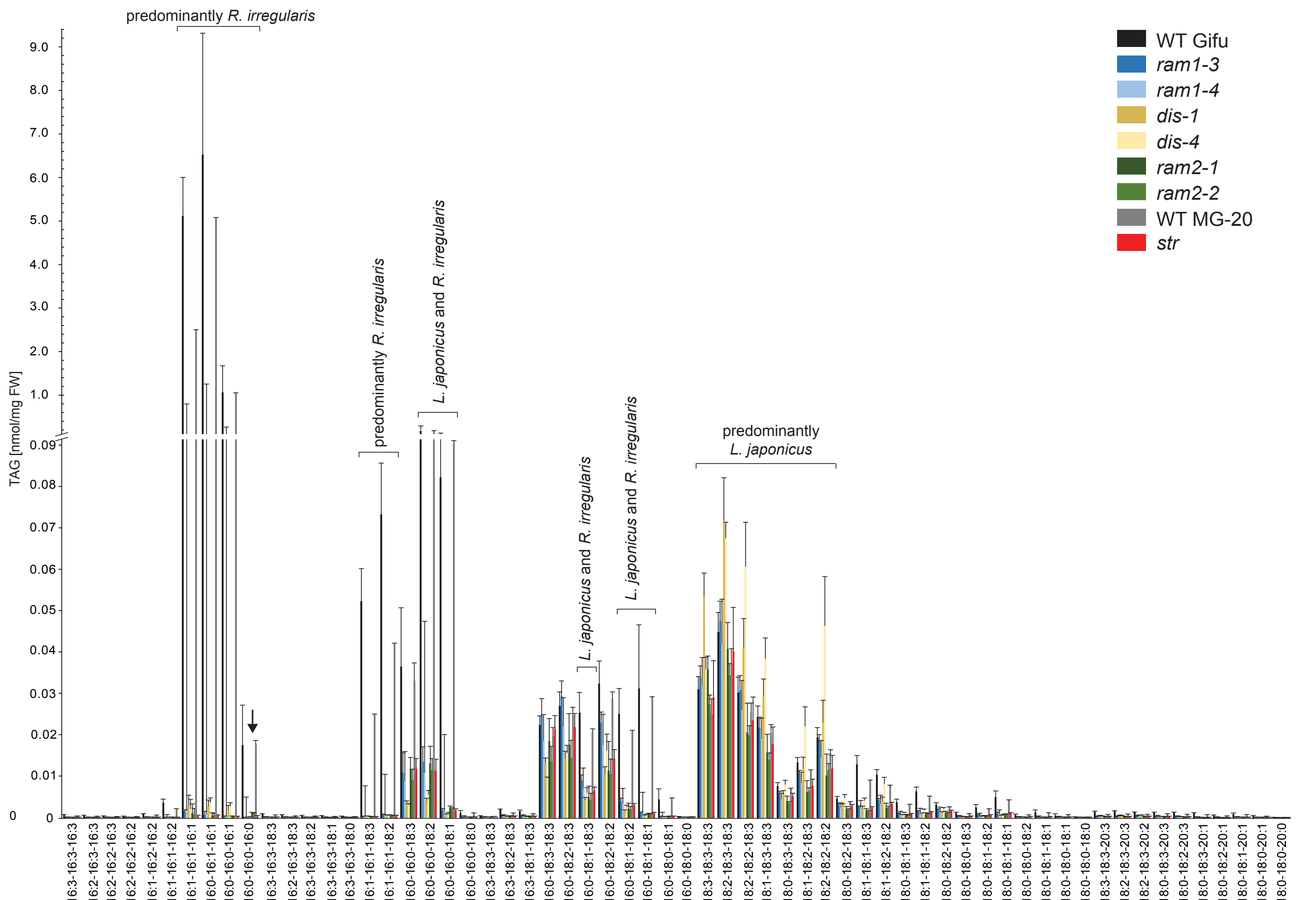

Figure 5—figure supplement 6. Triacylglycerol (TAG) profiles of colonized *L. japonicus* WT and AM-defective mutant roots. Absolute amounts of triacylglycerol molecular species in colonized *L. japonicus* roots of WT Gifu, WT MG-20 *ram1-3*, *ram1-4*, *dis-1*, *dis-4*, *ram2-1*, *ram2-2* and *str*. Black arrow indicates accumulation of tri 16:0 TAG in *ram2-1* and *ram2-2*. Bars represent means ±standard deviation (SD) of 3–5 biological replicates.
DOI: 10.7554/eLife.29107.029

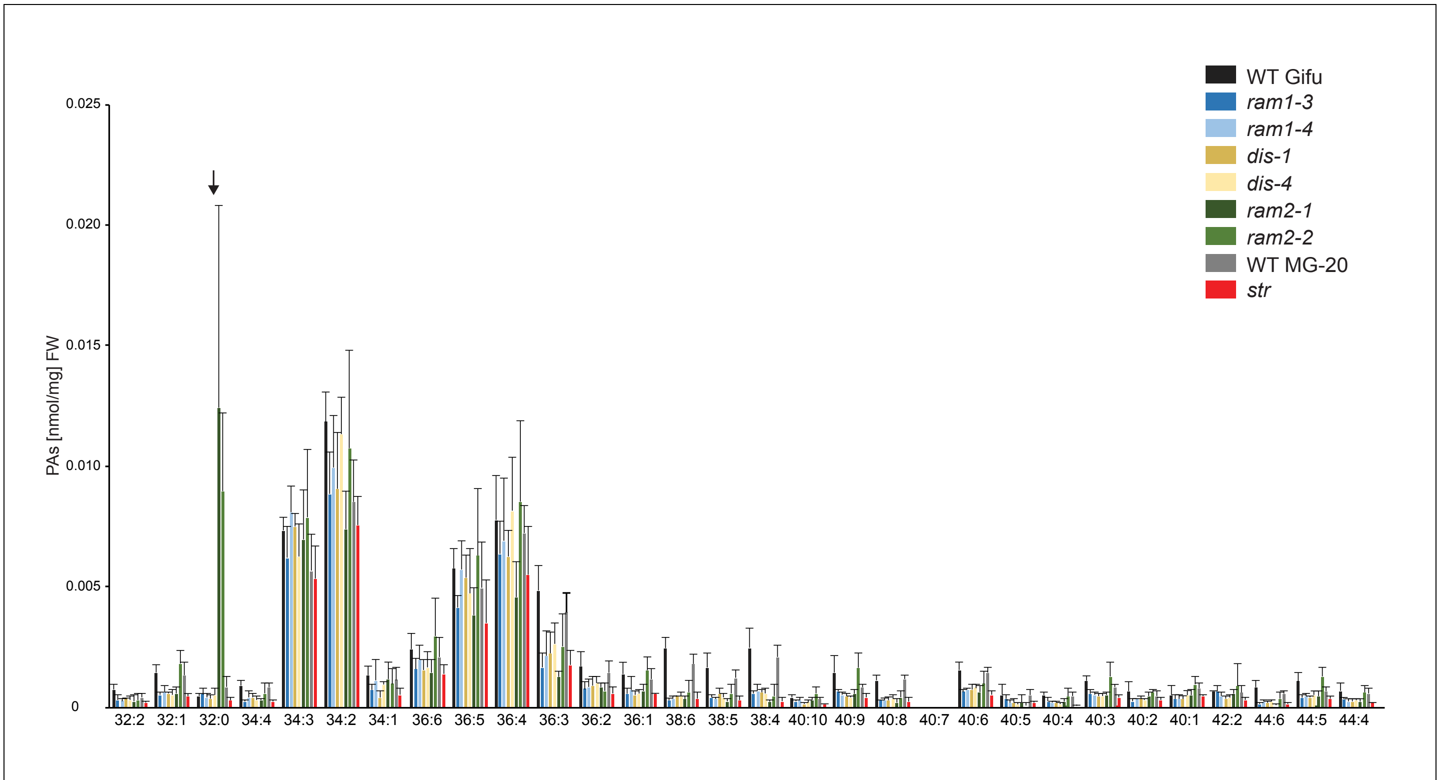

Figure 5—figure supplement 7. Phosphatidic acid (PA) profiles in *L. japonicus* WT and AM-defective mutants. Absolute amounts of phosphatidic acid molecular species in colonized *L. japonicus* roots of WT Gifu, WT MG-20 *ram1-3, ram1-4, dis-1, dis-4, ram2-1, ram2-2* and *str*. Black arrow indicates accumulation of 32:0 (di16:0) PA in *ram2-1* and *ram2-2.* Bars represent means ±standard deviation (SD) of 3–5 biological replicates.
DOI: 10.7554/eLife.29107.030

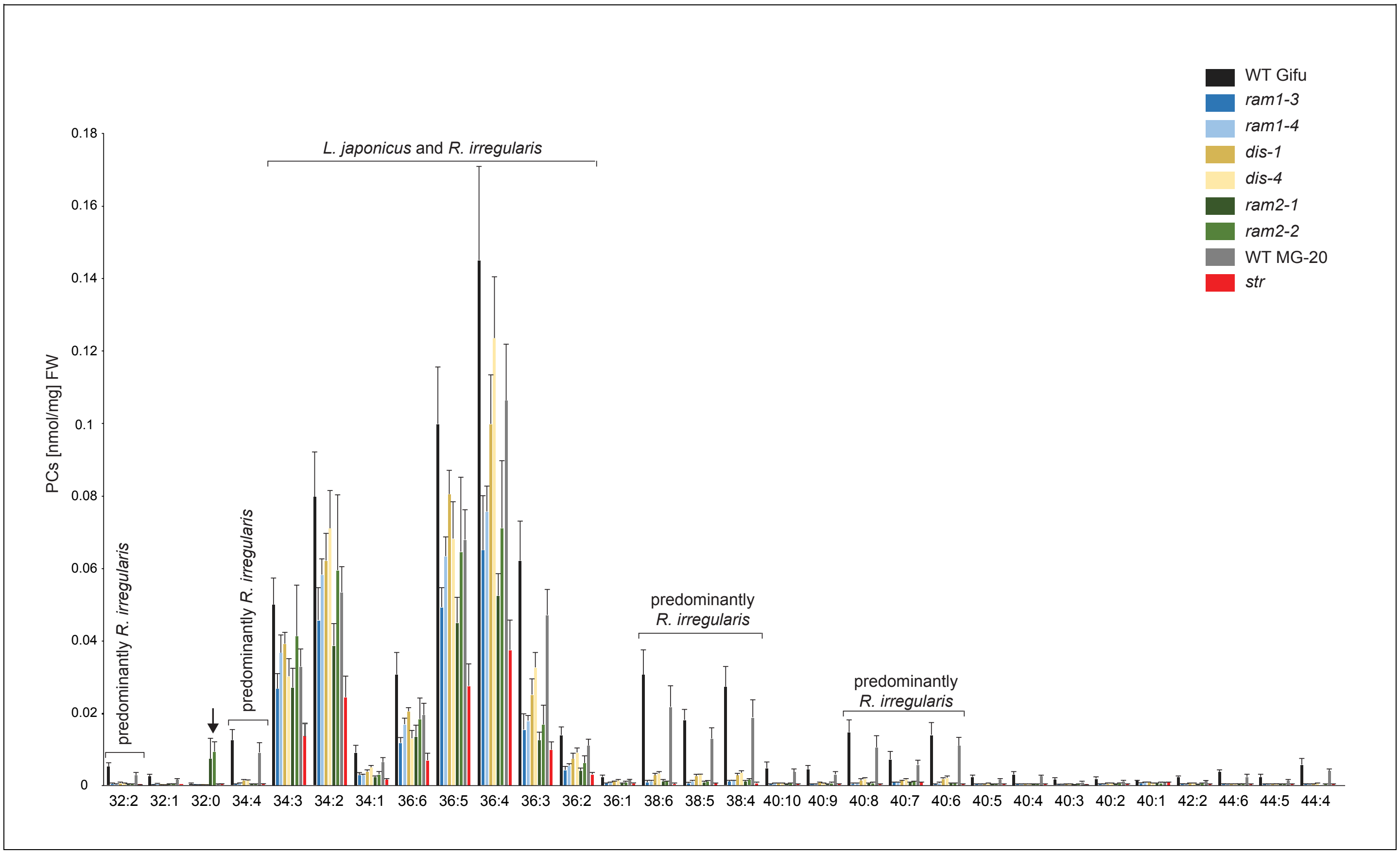

Figure 5—figure supplement 8. Profile of phosphatidylcholines (PC) in *L. japonicus* WT and AM-defective mutants. Absolute amounts of phosphatidylcholine molecular species in colonized *L. japonicus* roots of WT Gifu, WT MG-20, *ram1-3, ram1-4, dis-1, dis-4, ram2-1, ram2-2* and *str*. Bars represent means ±standard deviation (SD) of 3–5 biological replicates. '*L. japonicus* and *R. irregularis*' marks lipids which are found in both organisms according to ***Wewer et al. (2014)***. Arrow highlights the exclusive accumulation of unusual 32:0 (di16:0) PC in *ram2-1* and *ram2-2*.
DOI: 10.7554/eLife.29107.031

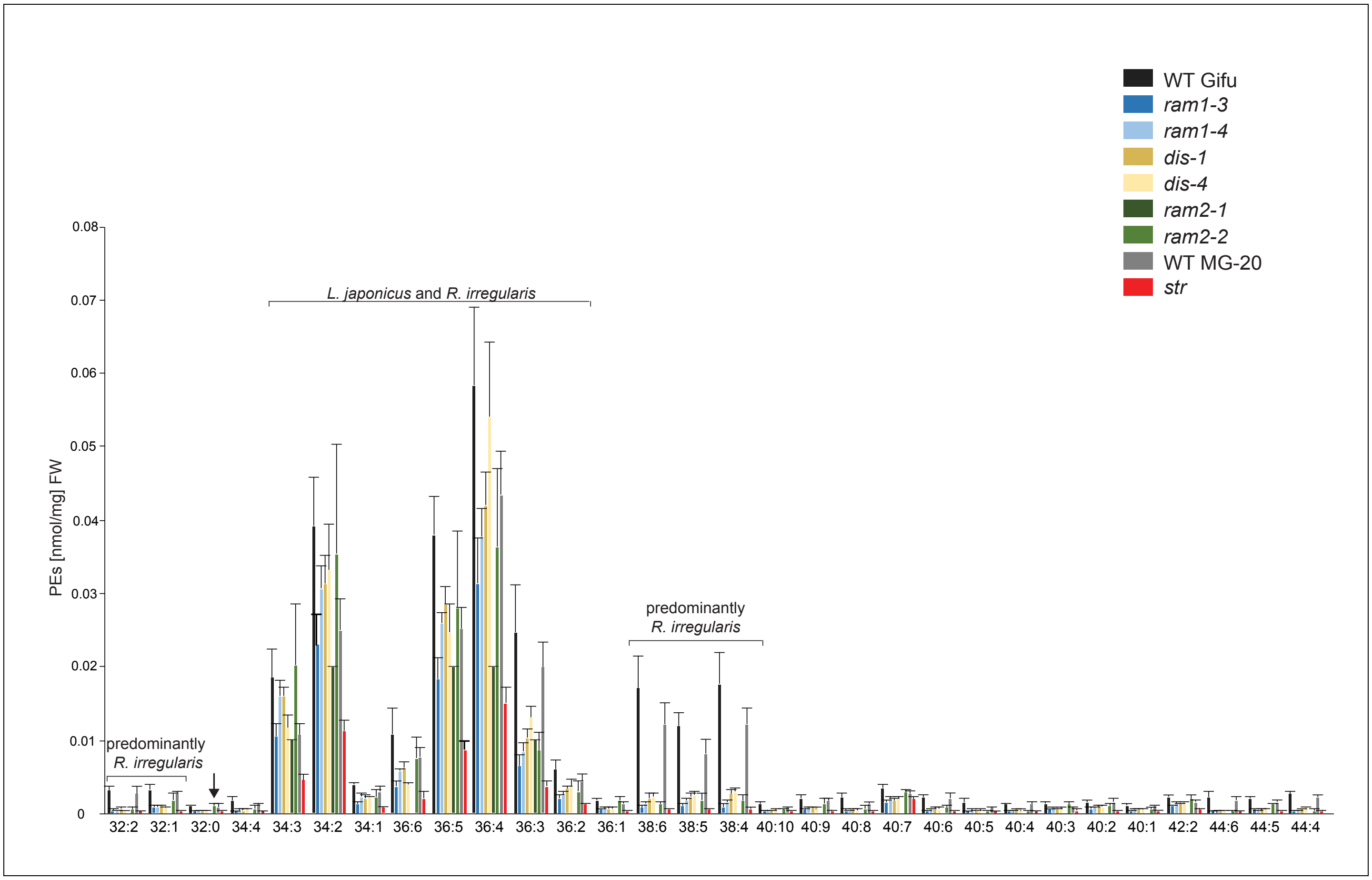

Figure 5—figure supplement 9. Phosphatidylethanolamine (PE) profile in *L. japonicus* WT and AM-defective mutants. Absolute amounts of phosphatidylethanolamine molecular species in colonized *L. japonicus* roots of WT Gifu, WT MG-20, *ram1-3, ram1-4, dis-1, dis-4, ram2-1, ram2-2* and *str*. Bars represent means ±standard deviation (SD) of 3–5 biological replicates. '*L. japonicus* and *R. irregularis*' marks lipids which are found in both organisms according to ***Wewer et al. (2014)***. Arrow highlights the exclusive accumulation of unusual 32:0 (di16:0) PE in *ram2-1* and *ram2-2*.
DOI: 10.7554/eLife.29107.032

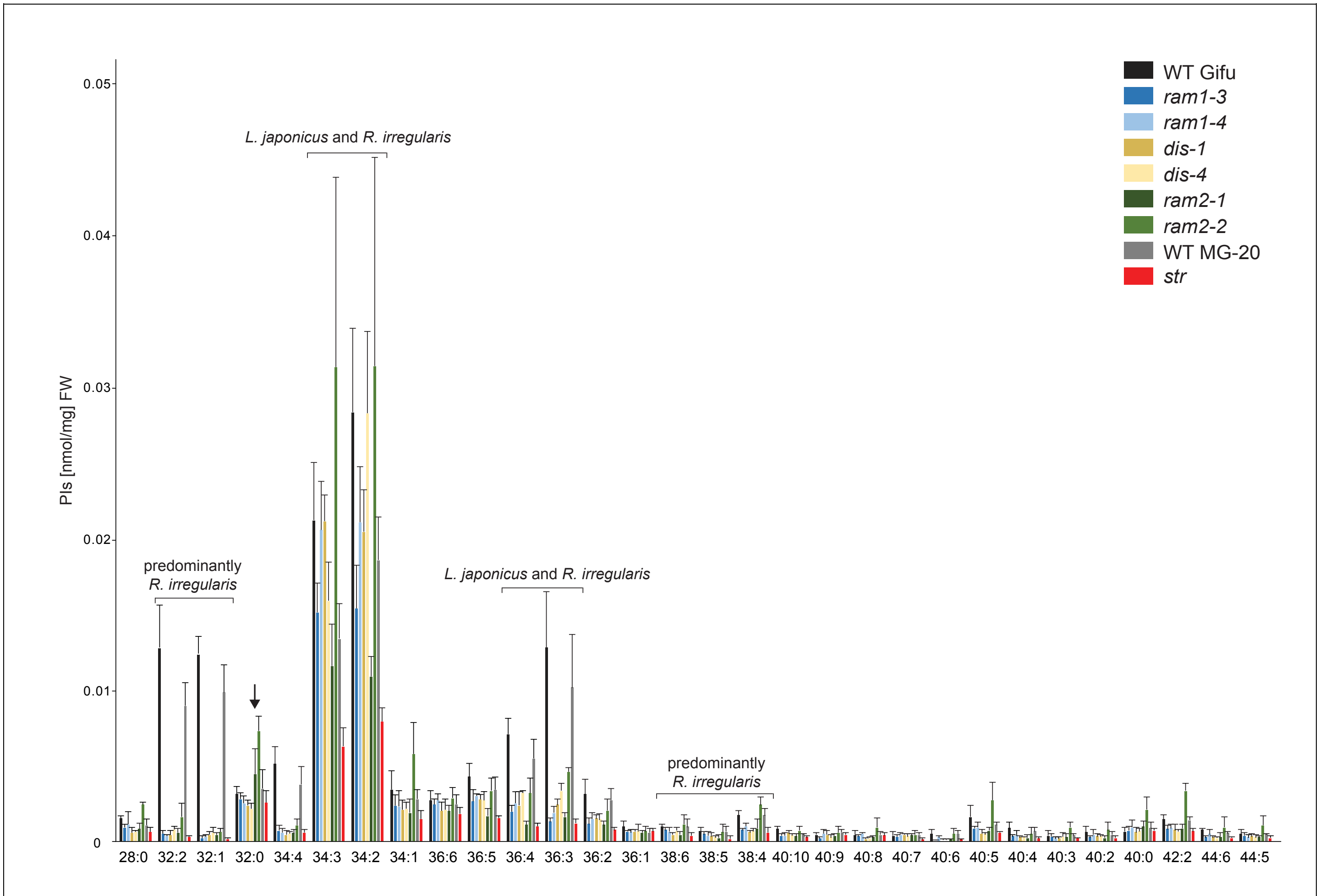

Figure 5—figure supplement 10. Phosphatidylinositol (PI) profile in *L. japonicus* WT and AM-defective mutants. Absolute amounts of phosphatidylinositol molecular species in colonized *L. japonicus* roots of WT Gifu, WT MG-20, *ram1-3*, *ram1-4*, *dis-1*, *dis-4*, *ram2-1*, *ram2-2* and *str*. Bars represent means ± standard deviation (SD) of 3–5 biological replicates. '*L. japonicus* and *R. irregularis*' marks lipids which are found in in both organisms according to ***Wewer et al. (2014)***. Arrow highlights the exclusive accumulation of unusual 32:0 PI in *ram2-1* and *ram2-2*.
DOI: 10.7554/eLife.29107.033

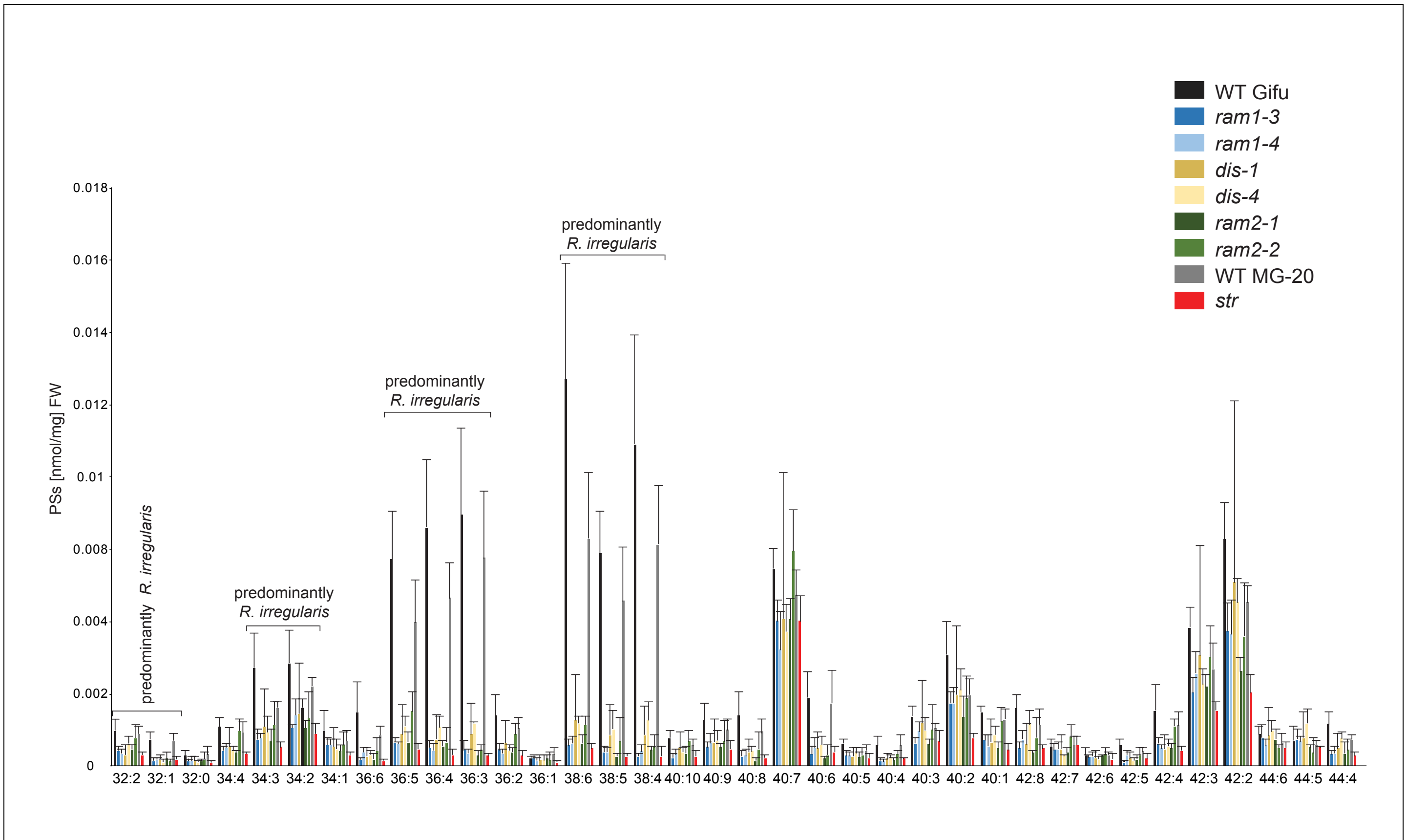

Figure 5—figure supplement 11. Phosphatidylserine (PS) profile in *L. japonicus* WT and AM-defective mutants. Absolute amounts of phosphatidylserine molecular species in colonized *L. japonicus* roots of WT Gifu WT, WT MG-20, *ram1-3, ram1-4, dis-1, dis-4, ram2-1, ram2-2* and *str*. Bars represent means ± standard deviation (SD) of 3–5 biological replicates.

DOI: 10.7554/eLife.29107.034

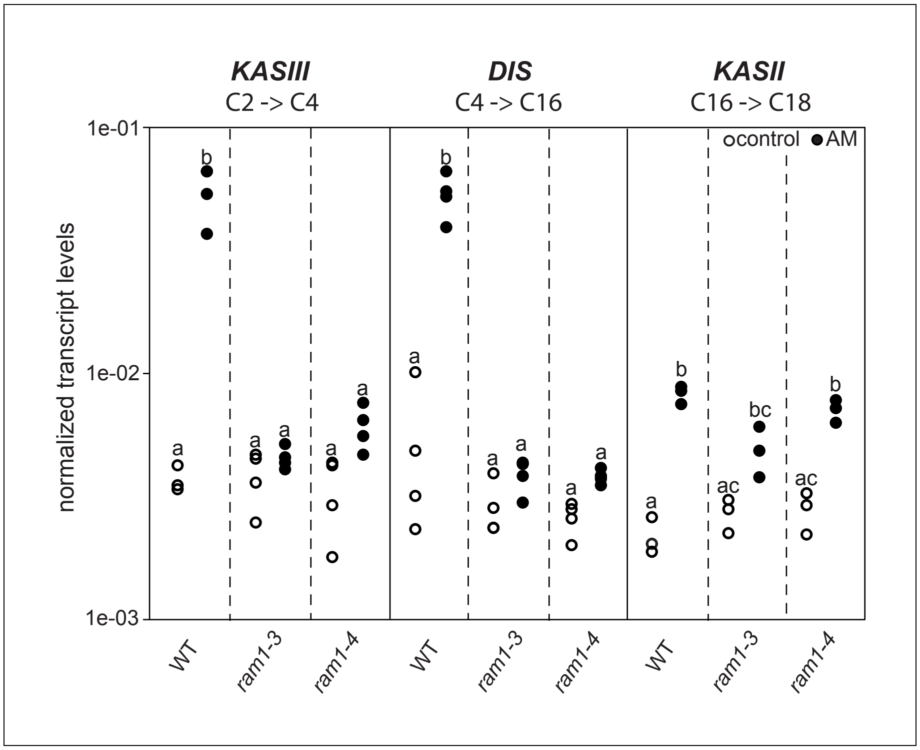

Figure 6. Loss of *RAM1* affects AM-dependent induction of *KASIII* and *DIS*. (**A**) *RAM1* effects on AM-dependent induction of *KASIII* and *DIS*, which catalyze 16:0 FA biosynthesis, and absence of effects on KASII. According to BLAST analysis via Kazusa (http://www.kazusa.or.jp/lotus/) and NCBI (http://www.ncbi.nlm.nih.gov/) *KASIII* and *KASII* are single copy genes in *L.japonicus*. Transcript accumulation of *KASIII, DIS* and *KASII* in non-colonized (open circles) and colonized (black circles) roots of Gifu WT, *ram1-3* and *ram1-4*. Different letters indicate different statistical groups (ANOVA; posthoc Tukey; $p \leq 0.001$; n = 23 $F_{5,12}$ = 65.04(*KASIII*); n = 24 $F_{5,18}$ = 54.42 (*DIS*); n = 18 $F_{5,12}$ = 33.11 (*KASII*)). Transcript accumulation was determined by qRT-PCR and the housekeeping gene *Ubiquitin10* was used for normalization. AM plants were inoculated with *R. irregularis* and harvested 5 wpi.
DOI: 10.7554/eLife.29107.035

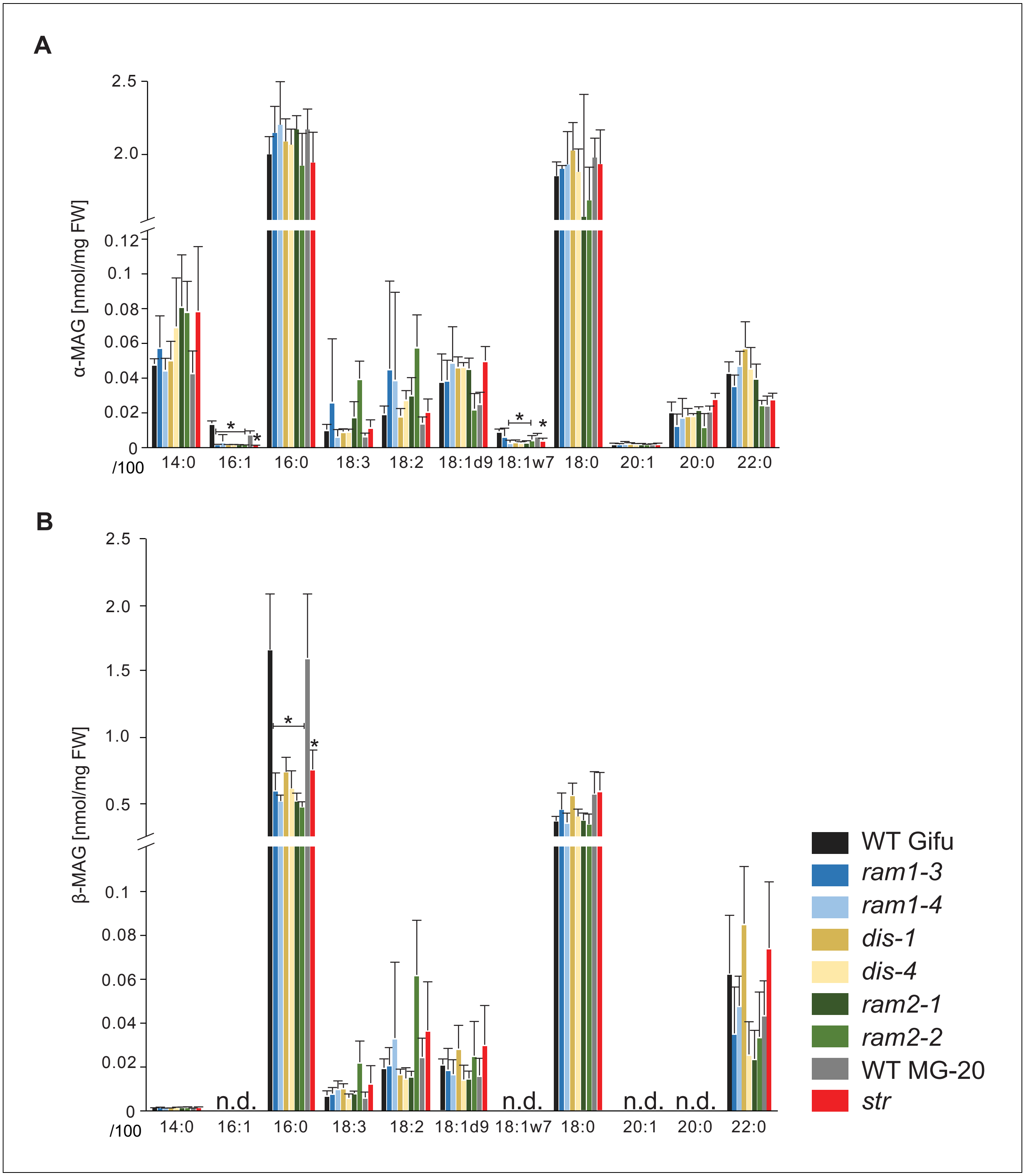

Figure 7. *sn-1* monoacylglycerol (α-MAG) and *sn-2* monoacylglycerol (β-MAG) profiles of colonized *L. japonicus* wild-type and AM-defective mutant roots. (**A**) Total amounts of α-MAG molecular species in the different genotypes. (**B**) Total amounts of β-MAG molecular species in the different genotypes. 16:0 β-MAG levels are significantly reduced in all mutant lines compared to the respective wild-type. (**A–B**) Bars represent means ±standard deviation (SD) of 3–5 biological replicates. Black asterisk indicates significant difference of mutants vs. wild-type according to Student's t-test, $p<0.05$.

DOI: 10.7554/eLife.29107.036

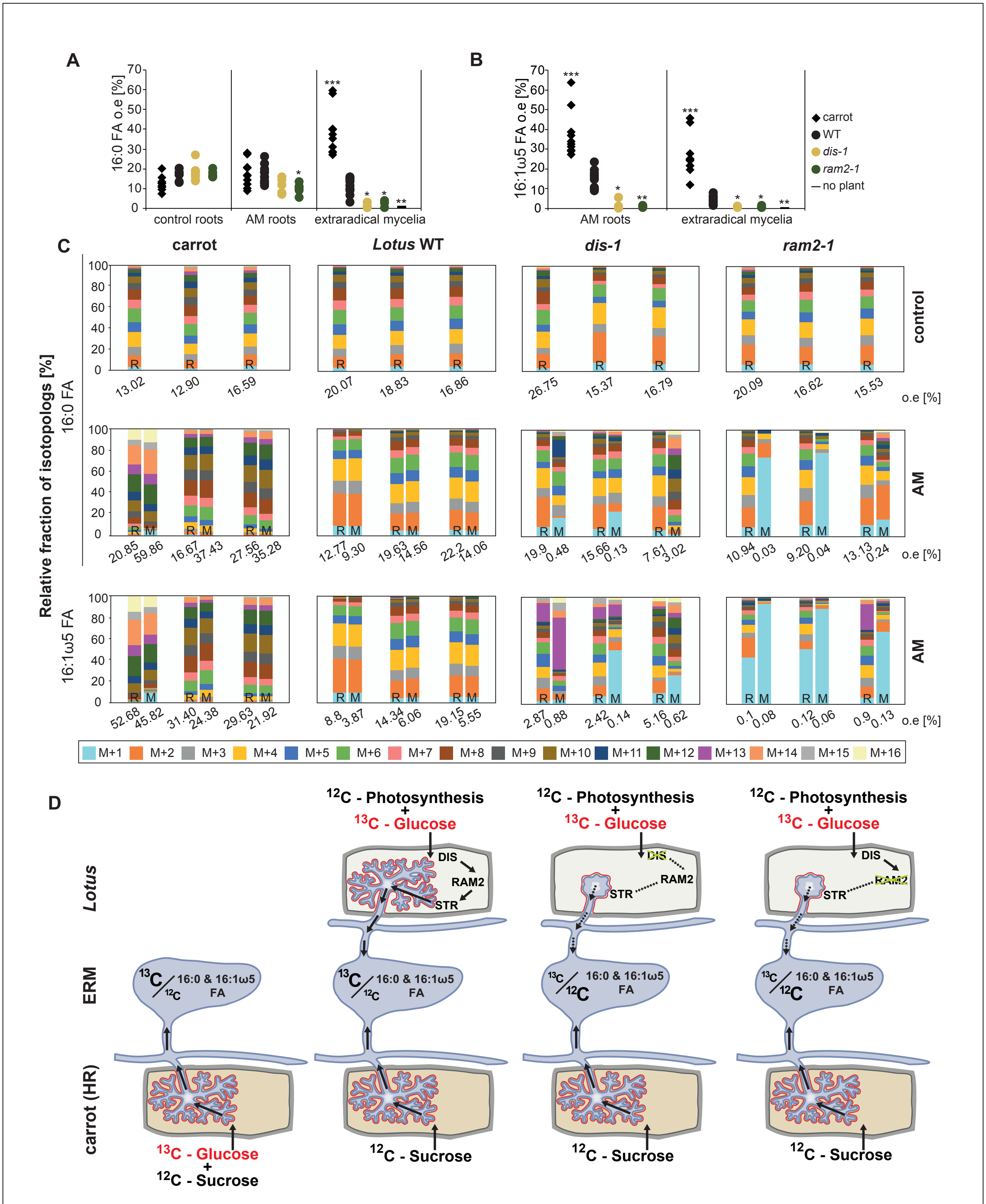

Figure 8. Isotopolog profiling indicates lipid transfer from plant to fungus. (A–B) Overall excess (o.e.) ^{13}C over air concentration in 16:0 FAs (A) and in 16:1ω5 FAs (B) detected in non-colonized (only 16:0 FAs) and colonized carrot, *L. japonicus* wild-type, *dis-1*, *ram2-1* roots and in the extraradical

Figure 8 continued on next page

Figure 8 continued

mycelium of *R. irregularis.* P values were generated by ANOVA using the Dunnett Test for multiple comparisons to *L. japonicus* wild-type (n = 29 (16:0 control roots); n = 33 (16:0 root AM); n = 39 (16:0 extraradical mycelium); n = 33 (16:1ω5 root AM); n = 39 (16:1ω5 extraradical mycelium), ***p<0.001, **p<0.01, *p<0.05). (**C**) Relative fraction of ^{13}C isotopologs for 16:0 FAs of three replicates of carrot, *L. japonicus* WT Gifu, *dis-1*, *ram2-1* in control roots (upper panel) and AM roots and each of the associated *R. irregularis* extraradical mycelia with spores (middle panel) and 16:1ω5 FAs in AM roots and extraradical mycelia with spores (lower panel). Individual bars and double bars indicate individual samples. Values from roots are indicated by 'R' and from fungal extraradical mycelia with spores by 'M'. For carrot and *L. japonicus* WT the ^{13}C labelling pattern of 16:0 and 16:1ω5 FAs in the plant is recapitulated in the fungal extraradical mycelium. Extraradical mycelium associated with *dis-1* and *ram2-1* does not mirror these patterns. Compare bars for AM roots and extraradical mycelium side by side. Black numbers indicate ^{13}C o. e. for individual samples. Colors indicate ^{13}C-isotopologs carrying one, two, three, etc. ^{13}C-atoms (M + 1, M + 2, M + 3, etc.). (**D**) Schematic and simplified illustration of carbon flow and ^{12}C vs. ^{13}C-carbon contribution to plant lipid metabolism and transport to the fungus in the two-compartment cultivation setup used for isotope labelling. Carbohydrate metabolism and transport is omitted for simplicity. ERM, extraradical mycelium.

DOI: 10.7554/eLife.29107.037

The following source data is available for figure 8:

Source data 1. Raw data for isotopolog profiles in ***Figure 8*** and ***Figure 8—figure supplements 2,4***.

DOI: 10.7554/eLife.29107.038

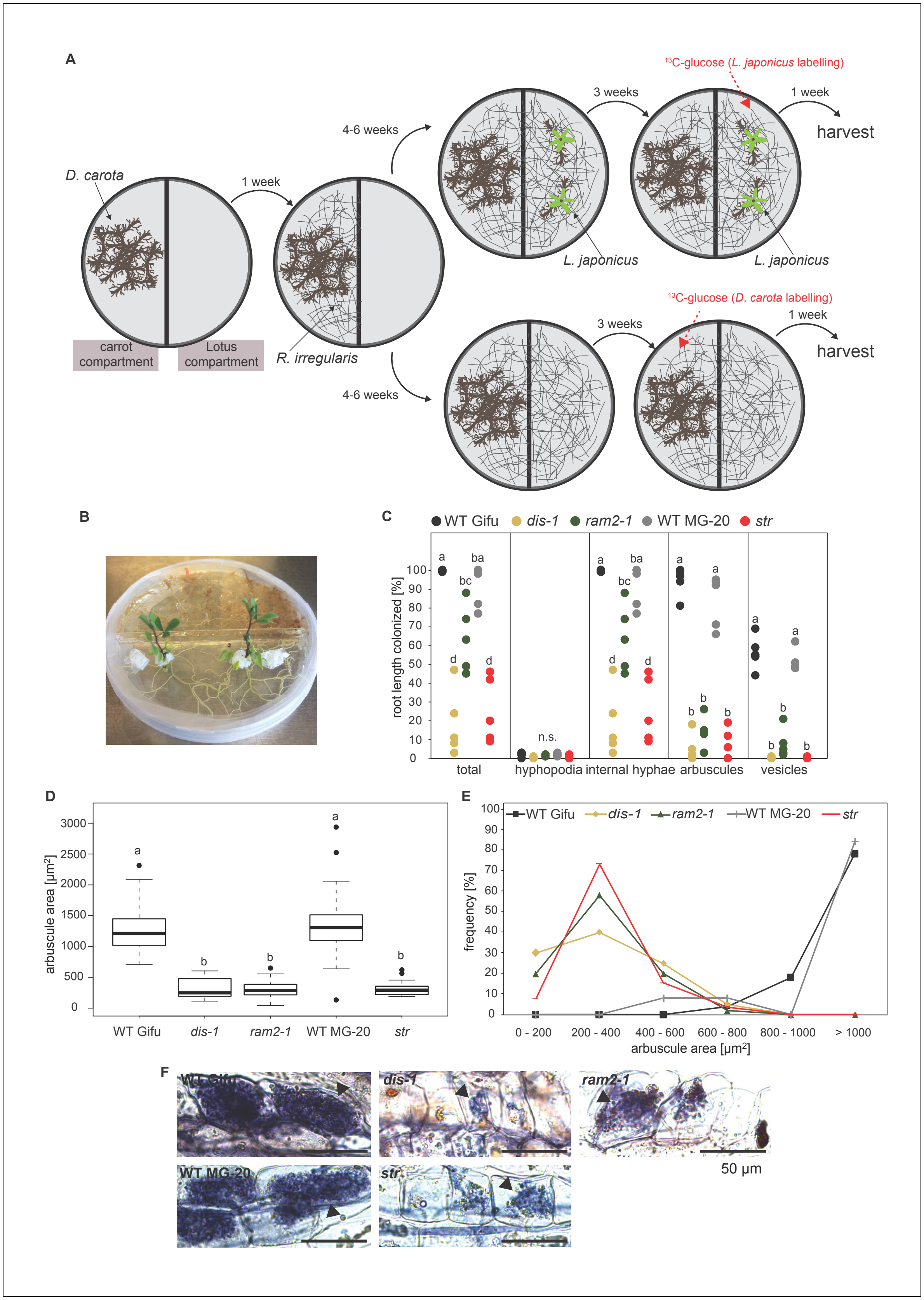

Figure 8—figure supplement 1. Two-compartment cultivation setup used for labelling experiments. (A) Schematic representation of cultivation setup which was used for ^{13}C-glucose labelling experiments (***Figure 8***, ***Figure 8—figure supplement 2–4***). [U-$^{13}C_6$]Glucose as substrate was either applied

Figure 8—figure supplement 1 continued on next page

Figure 8—figure supplement 1 continued

to the carrot compartment or the *Lotus* compartment. Colonized roots and extraradical mycelia populating the plate were harvested separately. (**B**) Photo of the 2-compartment setup. 2 week old *Lotus* seedlings were cultivated for 4 weeks on this setup. 100 mg of [U-$^{13}C_6$]Glucose was applied one week before harvest. (**C**) Quantitative AM colonization as determined by the modified grid-line intersect method after acid-ink staining in roots of genotypes indicated in the figure from plants grown in the Petri dish system (**A and B**) in parallel with the plants used for isotopolog profiling. Different letters indicate significant differences (ANOVA; posthoc Tukey; n = 25) among genotypes for each fungal structure separately. $p \leq 0.01$, $F_{4,20} = 32.49$ (total and intraradical hyphae); $F_{4,20} = 110.1$ (arbuscules), $F_{4,20} = 112.6$ (vesicles). (**D**) Arbuscule area and (**E**) frequency distribution of arbuscule area in the root samples used in (**C**). 10 arbuscules were analysed per root system. For wild-type Gifu, MG20 and *ram2-1* five, for *str* three and for *dis-1* two root systems were available. Different letters in (**D**) indicate significant differences (ANOVA; posthoc Tukey; n = 196) in arbuscule area among genotypes. $p \leq 0.001$, $F_{4,191} = 127.4$. (**E**) Representative bright-field images of arbuscules in roots of the samples analyzed in C-D.

DOI: 10.7554/eLife.29107.039

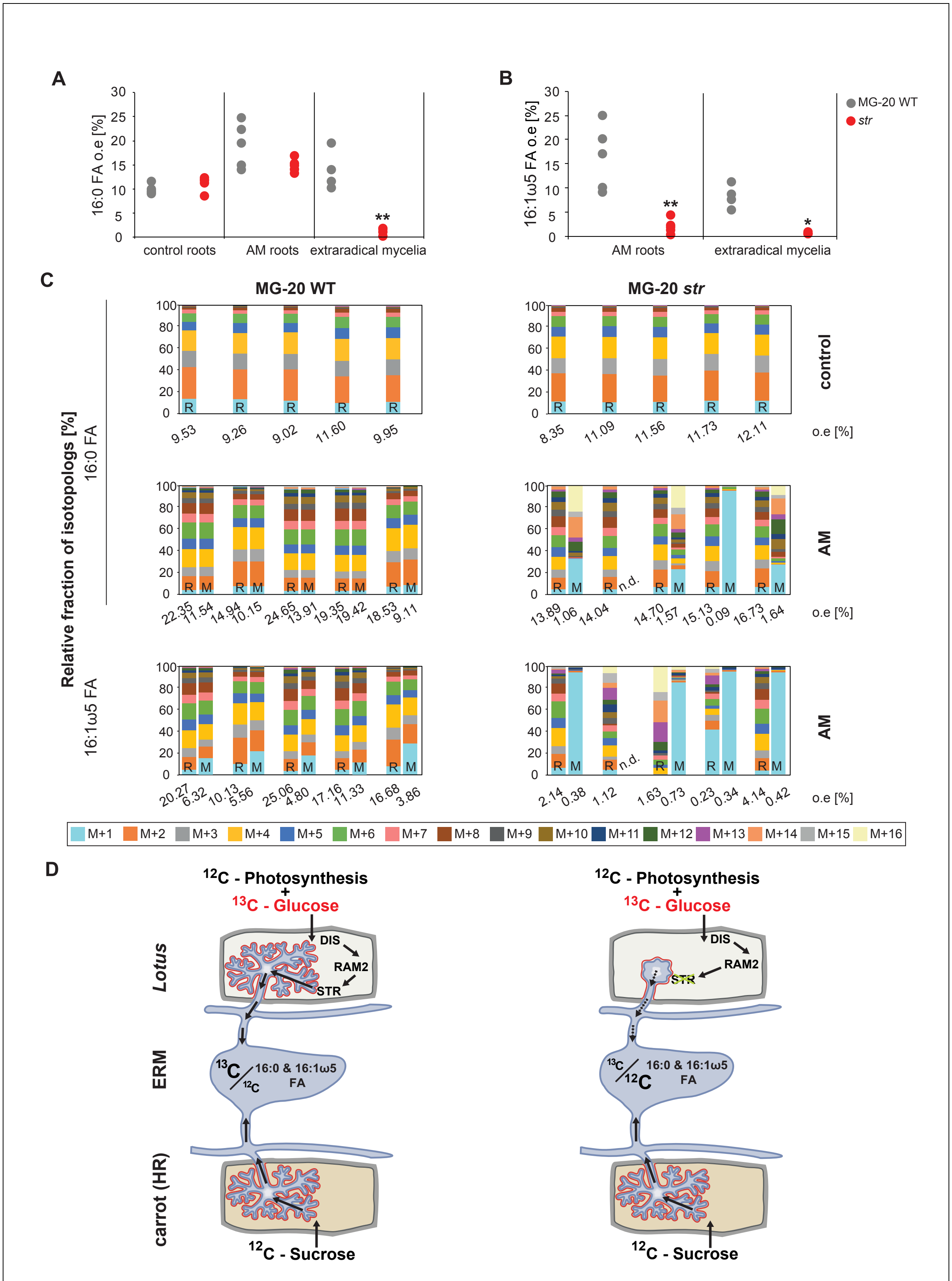

Figure 8—figure supplement 2. Isotopolog profiles of wild-type MG20 and *str*. (A–B) Overall excess (o.e.) of ^{13}C over air concentration in 16:0 FAs (A) and in AMF specific 16:1ω5 FAs (B) detected in non-colonized (only 16:0 FAs) and colonized, *L. japonicus* wild-type and *str* roots and in the extraradical

Figure 8—figure supplement 2 continued on next page

Figure 8—figure supplement 2 continued

mycelium of *R. irregularis.* Five biological replicates of each genotype and treatment are shown. Black asterisks indicate statistically significant differences between mutant lines and wild-type according to Student's t-test *$p<0.05$; **$p<0.01$. (**C**) Relative fraction of ^{13}C isotopologs for 16:0 fatty acids of five replicates (individual bars and double bars) of *L. japonicus* WT MG-20 and *str* in control roots (upper panel) and AM roots and each of the associated *R. irregularis* extraradical mycelia (middle panel). The same is shown for fungus-specific 16:1ω5 FAs in AM roots and extraradical mycelia (lower panel). Values from roots are indicated by 'R' and from fungal extraradical mycelia by 'M'. For *L. japonicus* wild-type the ^{13}C labelling pattern of 16:0 and 16:1ω5 FAs in the plant is recapitulated in the fungal extraradical mycelium. Extraradical hyphae associated with *str* do not mirror these patterns. Compare bars for AM roots and extraradical hyphae side by side. Black numbers indicate ^{13}C overall excess for individual samples. Colors indicate ^{13}C-isotopologues carrying one, two, three, etc. ^{13}C-atoms (M + 1, M + 2, M + 3, etc.). (n. d. = not detected). (**D**) Schematic and simplified illustration of carbon flow and ^{12}C vs.^{13}C contribution to plant lipid metabolism and transport to the fungus in the two-compartment cultivation setup used for isotope labelling. Carbohydrate metabolism and transport is omitted for simplicity. ERM, extraradical mycelium.

DOI: 10.7554/eLife.29107.040

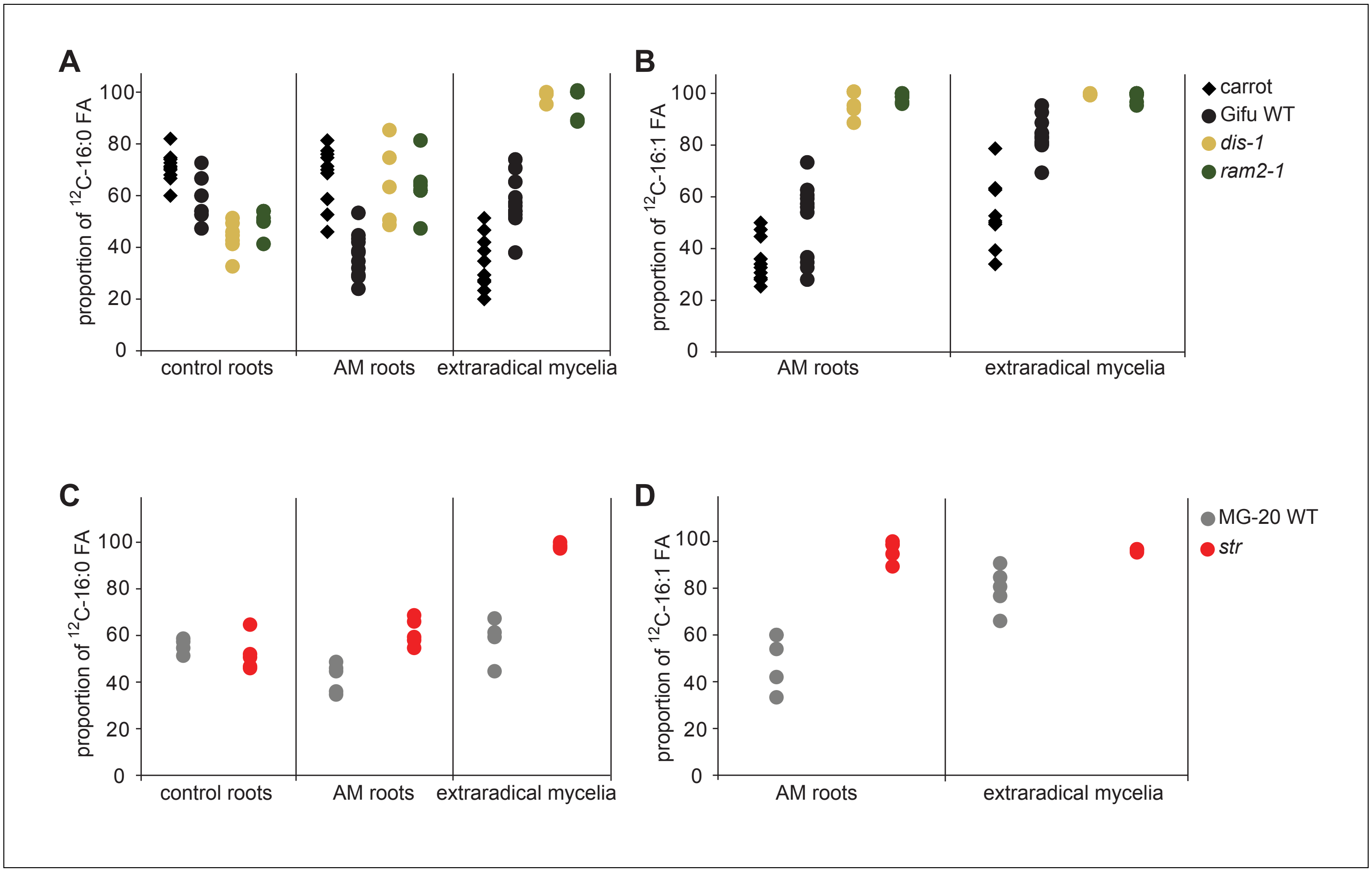

Figure 8—figure supplement 3. Proportion of 16:0 and 16:1ω5 FA containing only non-labelled ^{12}C in plant and fungal tissue. Proportion of ^{12}C 16:0 fatty acids (M + 0) in non-colonized and colonized carrot, *L. japonicus* Gifu wild-type, *dis-1*, *ram2-1* roots and in the extraradical mycelium of *R. irregularis* (**A**) as well as in *L. japonicus* MG-20 wild-type, *str* roots and in the extraradical mycelium of *R.irregularis* (**C**). Proportion of non-labeled ^{12}C AMF specific 16:1ω5 fatty acids (M + 0) in colonized carrot, *L. japonicus* Gifu wild-type, *dis-1*, *ram2-1* roots and in the extraradical mycelium of *R. irregularis* (**B**) as well as in *L. japonicus* MG-20 wild-type, *str* and in the extraradical mycelium of *R. irregularis* (**D**).
DOI: 10.7554/eLife.29107.041

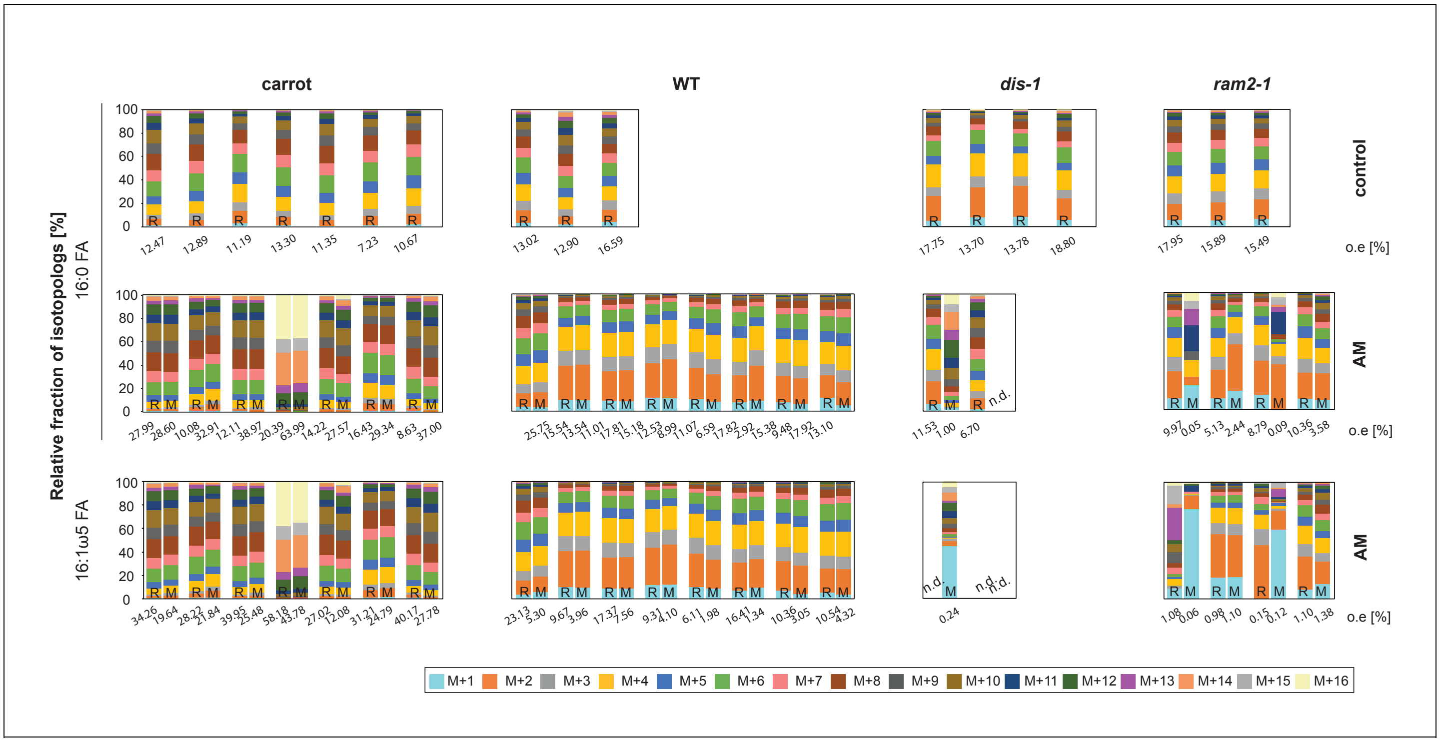

Figure 8—figure supplement 4. Isotopolog profiles of additional samples. Relative fraction of ^{13}C isotopologs for 16:0 fatty acids (individual bars and double bars) of *D. carota*, *L. japonicus* WT Gifu, *dis-1*, *ram2-1* in control roots (upper panel) and AM roots and each of the associated *R. irregularis* extraradical mycelia (middle panel) and 16:1ω5 FAs in AM roots and extraradical mycelia (lower panel). Values from roots are indicated by 'R' and from fungal extraradical mycelia by 'M'. Compare bars for AM roots and extraradical hyphae side by side. Isotopolog profiles shown here and in ***Figure 8C*** were generated from 3 independent experiments for *L. japonicus* wild-type and, 2 independent experiments for *L. japonicus* mutants and carrot roots. Transfer of ^{13}C-label from plant to fungus is higher for carrot than for *L. japonicus* wild-type. This is possibly caused by the fungus being exclusively dependent on carrot when carrot is labelled, while lipid transfer from *L. japonicus* competes with un-labeled transfer from carrot from the other side of the petri dish. Whatever the isotopolog pattern of wild-type roots, it is mirrored in the extrarical fungal mycelium, indicating lipid transfer. However, the isotopolog pattern is for most cases not mirrored in extraradical mycelium associated with lipid biosynthesis mutants. (n.d. = not detected).

DOI: 10.7554/eLife.29107.042

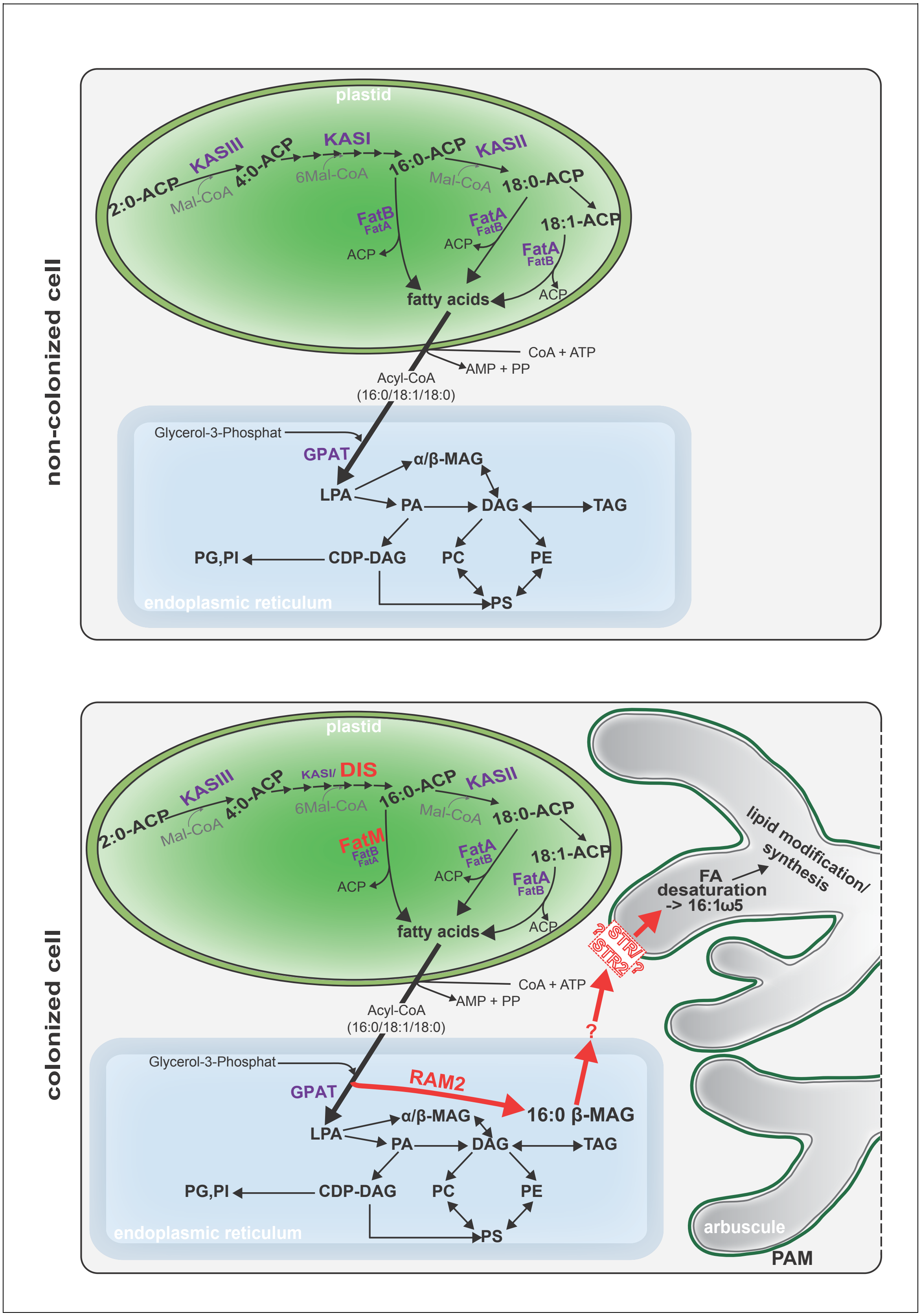

Figure 9. Schematic representation of plant fatty acid and lipid biosynthesis in a non-colonized root cell and a root cell colonized by an arbuscule. In non-colonized cells FAs are synthesized in the plastid, bound via esterification to glycerol to produce LPA in the ER, where further lipid synthesis and

Figure 9 continued on next page

Figure 9 continued

modification take place. Upon arbuscule formation AM-specific FA and lipid biosynthesis genes encoding DIS, FatM and RAM2 are activated to synthesize specifically high amounts of 16:0 FAs and 16:0-ß-MAGs or further modified lipids (this work and ***Bravo et al., 2017***). These are transported from the plant cell to the fungus. The PAM-localized ABCG transporter STR/STR2 is a hypothetical candidate for lipid transport across the PAM. Desaturation of 16:0 FAs by fungal enzymes (***Wewer et al., 2014***) leads to accumulation of lipids containing specific 16:1ω5 FAs. Mal-CoA, Malonyl-Coenzyme A; FA, fatty acid; KAS, β-keto-acyl ACP synthase; GPAT, Glycerol-3-phosphate acyl transferase; PAM, periarbuscular membrane; LPA, lysophosphatic acid; MAG, monoacylglycerol; DAG, diacylglycerol; TAG, triacylglycerol; PA, phosphatidic acid; PC, phosphatidylcholine; PE, phosphatidylethanolamine; PS, phosphatidylserine; CDP-DAG, cytidine diphosphate diacylglycerol; PG, phosphatidylglycerol; PI, phosphatidylinositol.
DOI: 10.7554/eLife.29107.043